Journal of Food Engineering 370 (2024) 111867

Contents lists available at ScienceDirect

Journal of Food Engineering

journal homepage: www.elsevier.com/locate/jfoodeng

Ingredient functionality in batter-type cake baking: Coupled multiphase poro-hygro-viscoelastic model

Kalayarasan Seranthian [a], Ashim Datta [a,*], Aaron Clanton [b]

[a] Department of Biological and Environmental Engineering, Cornell University, 208 Riley Robb Hall, Ithaca, NY 14853, USA
[b] Department of grain Science, Kansas State University, 107 Shellenberger Hall, Manhattan, KS 66506, USA

ARTICLE INFO

Keywords:
Cake baking
Multi-phase transport
Large-strain viscoelasticity
Ingredient functionality
Mechanistic modeling
Performance metrics prediction

ABSTRACT

Ingredients play a crucial role in cake baking, significantly impacting important metrics like oven rise, moisture content, and color. While there is existing knowledge, a comprehensive mechanistic understanding of the intricate relationships between ingredients and the underlying physics is needed. We use a porous media-based multiphase transport framework coupled with large-strain viscoelastic deformation to study how water, sugar, and fat influence cupcakes' height, weight, and color starting from the batter stage. We show that high water content batters have an expedited oven rise due to increased thermal diffusivity leading to faster heat transfer and higher evaporation rates but lower surface temperature relative to low water content batters and, thus, less browning. High sugar and high fat batters have a delayed batter-to-foam material transformation because of increased starch gelatinization temperature, leading to shorter and drier cupcakes because of higher vapor loss early in baking. We find that lowering water or increasing sugar or fat content in the batter gives darker cupcakes because of increased surface temperatures. The novel mechanistic understanding of ingredient functionality can extend to mechanistic understanding and optimization of other baking processes.

1. Introduction

Cake baking is a dynamic multiphysics process with complex interactions between the ingredients (Bennion and Bamford, 1997; Pyler and Gorton, 2008). Cake ingredients profoundly affect key performance metrics such as color, moisture content, and oven rise. A mechanistic knowledge of ingredient functionality is crucial for ingredient scaling/metering. Despite the baking industry's long history, the role of ingredients during the baking process still needs to be fully understood (Sablani et al., 1998; Jacob, 2007; Sumnu and Sahin, 2008; Feyissa et al., 2011; Sakin-Yilmazer et al., 2012; Wilderjans et al., 2013; Ureta et al., 2016; Godefroidt et al., 2019; Cevoli et al., 2020) and the current understanding is predominantly based on trial-and-error. Mechanistic knowledge of ingredient functionality aids in designing and optimizing products and processes in the baking industry based on scientific understanding. In this study, we develop a mechanistic understanding of the functionality of cake's three main ingredients: water, sugar, and fat

1.1. Objectives and overview

The objectives of this study are: (1) develop a porous media-based multiphase transport framework with large-strain viscoelasticity for baking an off-the-shelf cupcake recipe, (2) validate the multiphysics framework with experimentally measured cupcake metrics (oven rise, color, weight loss, internal temperatures), (3) provide a first principle-based mechanistic understanding of the ingredient functionality on the performance metrics of cupcakes, and (4) validate the understanding with experimentally measured cake height, weight and color for different batter compositions.

2. Model development

2.1. Physical processes in cake baking

This section presents a porous media-based multiphysics framework (Fig. 1) for baking (Seranthian and Datta, 2023) an off-the-shelf cupcake recipe with the assumptions, governing equations, and initial and boundary conditions. We did not simulate cooling outside the oven. The structure is set before the cake is taken out of the oven and is retained outside for the most part, with a small reduction in height, likely due to vapor loss, as it would be for any moist product. The general approach consisting of the governing equations and the property expressions would continue to be valid for this cooling portion as well. However, this period has minimal changes and was not in our interest. This may

* Corresponding author.
E-mail address: akd1@cornell.edu (A. Datta).

https://doi.org/10.1016/j.jfoodeng.2023.111867
Received 10 July 2023; Received in revised form 28 November 2023; Accepted 30 November 2023
Available online 7 December 2023

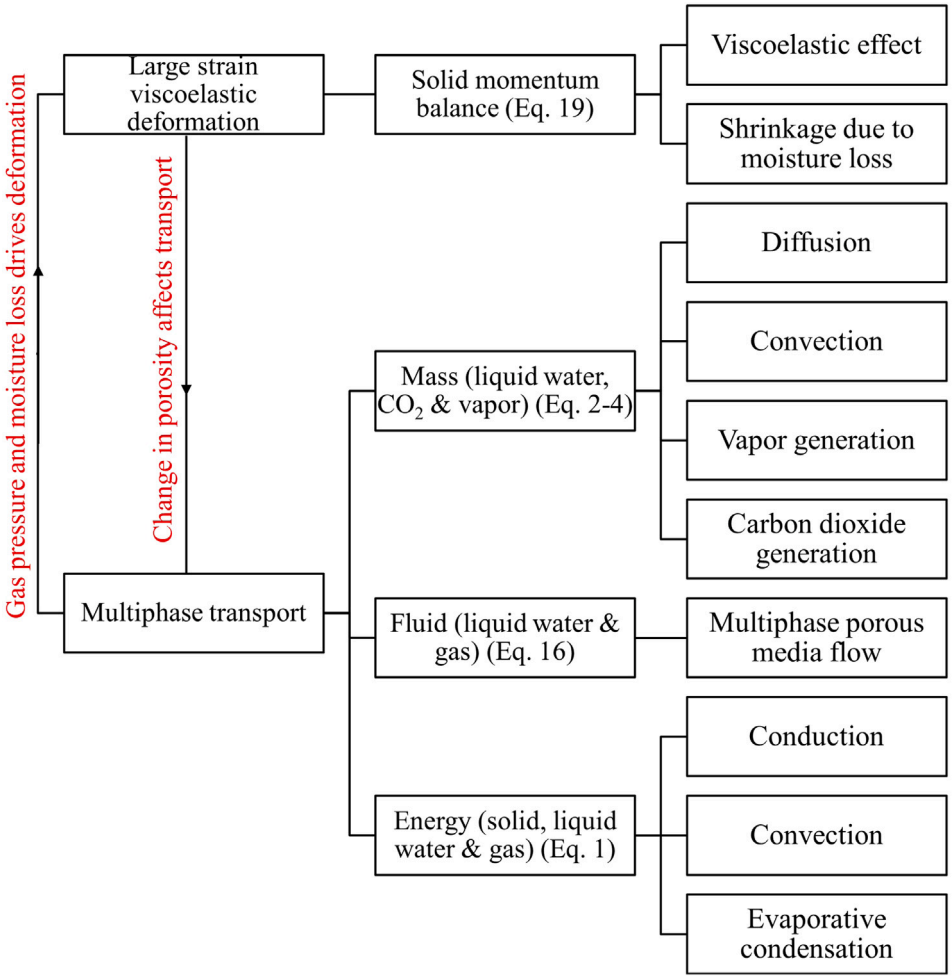

Fig. 1. The different physics involved in cake baking. Section 2.2 discusses the equations mentioned.

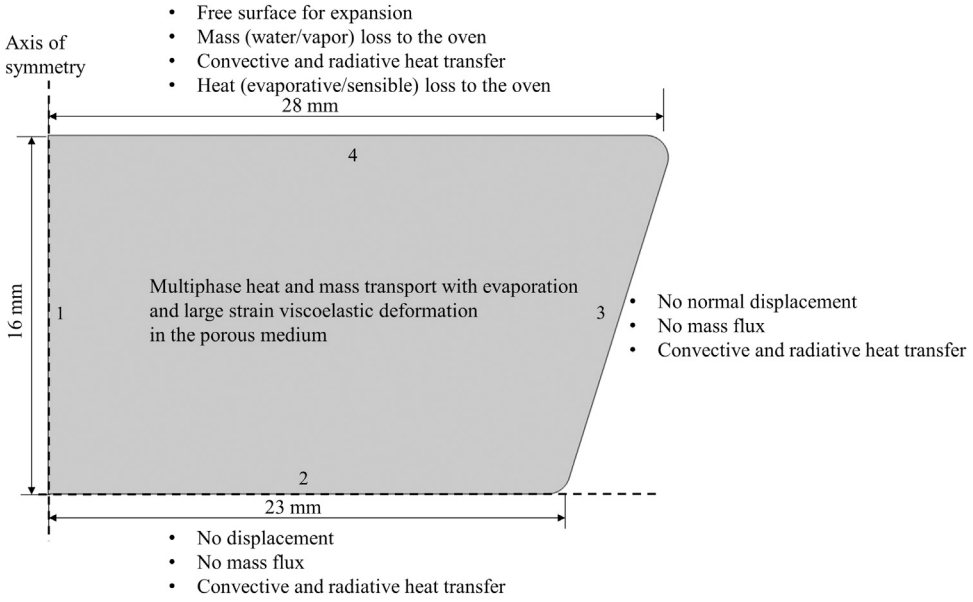

Fig. 2. Schematic showing the cupcake geometry and boundary conditions for the poro-hygro-viscoelastic model.

Table 1
Input parameters used in the cake baking simulation with additional details provided in Seranthian and Datta (2023).

Parameter	Value	Units	Source
Density			
Water, ρ_w	998	kg/m^3	McCabe et al. (1993)
Vapor, ρ_v	Ideal gas	kg/m^3	
Air, ρ_g	Ideal gas	kg/m^3	
Solid, ρ_s	$\frac{\rho_{0,eff}-\phi_0\rho_f}{1-\phi_0}$	kg/m^3	
Specific heat capacity			
Water, $C_{p,w}$	$4176.2-0.0909(T-273)+5.4731\times10^{-3}(T-273)^2$	J/kg K	Lewis (1990)
Vapor, $C_{p,v}$	$1790+0.107(T-273)+5.856\times10^{-4}(T-273)^2-1.997\times10^{-7}(T-273)^3$	J/kg K	Lewis (1990)
Air, $C_{p,a}$	$1004.828-0.01185(T-273)+4.3\times10^{-4}(T-273)^2$	J/kg K	Choi and Okos (1986)
Solid, C_{ps}	2200	J/kg K	Lostie et al. (2002)
Thermal conductivity			
Water, k_w	$0.57109+0.0017625T-6.7306\times10^{-6}T^2$	W/m K	Choi and Okos (1986)
Vapor, k_v	0.026	W/m K	Choi and Okos (1986)
Air, k_a	0.026	W/m K	Choi and Okos (1986)
Solid, k_s	0.12	W/m K	Lostie et al. (2004)
Intrinsic permeability			
Water, $k_{in,w}$	Fig. 3	m^2	Warning et al. (2014)
Air and vapor, $k_{in,g}$	$k_{in,w}\left(1+\frac{0.15k_{in,w}^{-0.37}}{p}\right)$	m^2	Tanikawa and Shimamoto (2009)
Relative permeability			
Water, $k_{r,w}$	$f(\phi)((S_w-0.09)/0.91)^3, S_w>0.09$ $0, S_w<0.09$		Bear (1988)
Air and vapor, $k_{r,g}$	$f(\phi)(1-1.1S_w), S_w<0.91$ $0, S_w>0.91$		Bear (1988)
Porosity factor, $f(\phi)$	$\left(\frac{\phi}{\phi_0}\right)^3\left(\frac{1-\phi_0}{1-\phi}\right)^2$		Bear (1988)
Capillary diffusivity			
Water, $D_{w,cap}$	$1.35\times10^{-8}\times\exp\left[\frac{-21.61(548-T)(1.194+3.68M)}{T(1+18.98M)}\right]$	m^2/s	van der Lijn (1976)
Vapor diffusivity			
In air, D_{bin}	$1.6\times10^{-5}(S_g\phi)^{4/3}$	m^2/s	Moldrup et al. (2005)
Viscosity			
Water, μ_w	0.988×10^{-3}	Pa s	McCabe et al. (1993)
Air and vapor, μ_g	1.8×10^{-5}	Pa s	McCabe et al. (1993)
Convective heat transfer coefficient, h_t	25	W/m^2 K	Sakin et al. (2007, 2009)
Radiative heat transfer coefficient, h_r	6	W/m^2 K	Sakin et al. (2007, 2009)
Mass transfer coefficient, h_m	0.01	m/s	
Latent heat of vaporization, λ	2.26×10^6	J/kg	Schwartzberg et al. (1995)
Equilibrium vapor pressure, $p_{v,eq}$	$a_w\times p_{v,sat}$	kPa	Basu et al. (2006) and Andrade et al. (2011)
Saturation vapor pressure, $p_{v,sat}$	$\exp\left(8.07131-\left[\frac{1730.63}{233.426+(T-273.15)}\right]\right), T\le373.15$ K $\exp\left(8.14019-\left[\frac{1810.94}{244.485+(T-273.15)}\right]\right), T>373.15$ K	kPa	Antoine (1888)
Water activity, a_w	Eq. (34)	–	Basu et al. (2006) and Andrade et al. (2011)
Elastic modulus, $E(T)$	Fig. 4(a)	Pa	
Relaxation time, $\tau(T)$	Fig. 4(b)	s	
Initial conditions			
Porosity, ϕ_0	0.5	–	Lostie et al. (2002)
Pressure, P_0	101,325	Pa	
Water concentration, $c_{w,0}$	$\rho_w S_{w,0}\phi_0$	kg/m^3	This study
Water saturation, $S_{w,0}$	$\frac{M_0(1-\phi_0)\rho_s}{\phi_0\rho_w}$	–	This study
Moisture, M_0	0.434	–	This study
Vapor mass fraction, $\omega_{v,0}$	$\frac{x_{v,0}M_v}{x_{v,0}M_v+(1-x_{v,0})M_{CO_2}}$, where $x_{v,0}=\frac{p_{v,eq}(T_0,M_0)}{p_0}$	–	This study
Temperature, T_0	20	°C	This study
Batter density, $\rho_{0,eff}$	856.26	kg/m^3	This study

also require mechanical properties data while the sample is cooled, which we did not collect.

2.2. Governing equations

Fig. 2 shows a schematic for the cake baking process. This section describes the governing equations for the coupled multiphase poro-hygro-viscoelastic deformation in the cake baking process.

2.2.1. Multiphase transport

Governing equations for porous media-based multiphase transport in cake baking are developed based on mass and energy conservation (Datta, 2007; Dhall and Datta, 2011; Seranthian and Datta, 2023):

$$\rho_{eff}C_{p,eff}\frac{\partial T}{\partial t}+\sum_{i=w,v,\mathrm{CO_2}}C_{p,i}(\vec{n}_i\cdot\nabla T)=\nabla\cdot(k_{eff}\nabla T)-\lambda\dot{I} \tag{1}$$

$$\frac{\partial c_w}{\partial t}+\nabla\cdot\vec{n}_{w,G}=-\dot{I} \tag{2}$$

$$\frac{\partial c_g}{\partial t}+\nabla\cdot\vec{n}_{g,G}=\dot{I}+\dot{R}_{\mathrm{CO_2}} \tag{3}$$

$$\frac{\partial c_v}{\partial t}+\nabla\cdot\vec{n}_{v,G}=\dot{I} \tag{4}$$

where the volumetric concentrations, c_i, of the three mass species (liquid water, gas, and water vapor) relate to the respective relative saturations, S_i, mass fractions in the gas phase, ω_i, and total porosity, ϕ, as follows:

$$c_w=\rho_w S_w\phi \tag{5}$$

$$c_g=\rho_g S_g\phi \tag{6}$$

$$c_v=\rho_g S_g\phi\omega_v \tag{7}$$

$$c_{\mathrm{CO_2}}=\rho_g S_g\phi\omega_{\mathrm{CO_2}} \tag{8}$$

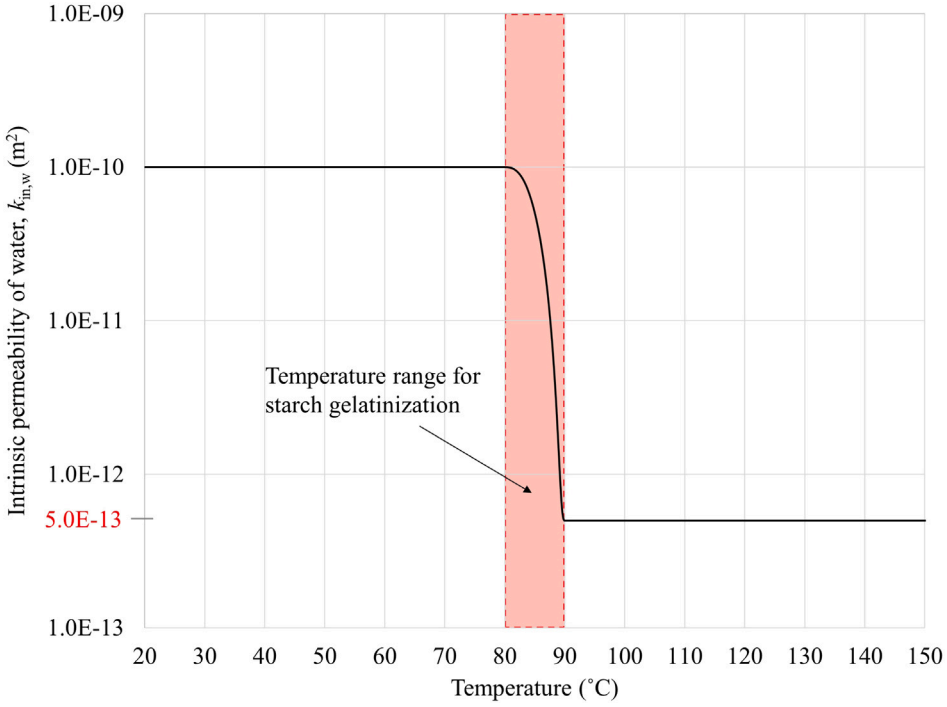

Fig. 3. Intrinsic permeability evolution with temperature (approximated, Section 2.5.1).

$$\omega_{CO_2} = 1 - \omega_v \tag{9}$$

It is assumed that the gas phase is a binary mixture of water vapor and carbon dioxide. The effective properties of the porous medium are given by:

$$\rho_{eff} = (1-\phi)\rho_s + \phi(S_w\rho_w + S_g\rho_g) \tag{10}$$

$$C_{p,eff} = m_s C_{p,s} + m_w C_{p,w} + m_g C_{p,g} \tag{11}$$

$$k_{eff} = (1-\phi)k_s + \phi(S_w k_w + S_g(\omega_v k_v + \omega_{CO_2} k_{CO_2})) \tag{12}$$

Eq. (1) solves for temperature and Eqs. (2)–(4) solve for the respective concentrations, c_w, c_g and c_v. The other unknowns, $\dot{I}$ and $\dot{R}_{CO_2}$, have separate equations discussed below. The mass fluxes in the ground frame are:

$$\vec{n}_{w,G} = \rho_w \vec{v}_{w,s} - D_{w,cap}\nabla c_w + c_w \vec{v}_s \tag{13}$$

$$\vec{n}_{g,G} = \rho_g \vec{v}_{g,s} + c_g \vec{v}_s \tag{14}$$

$$\vec{n}_{v,G} = \rho_v \vec{v}_{g,s} - \frac{C^2}{\rho_g} M_v M_{CO_2} D_{bin} \nabla x_v + c_v \vec{v}_s \tag{15}$$

where $\vec{v}_s$ is the velocity of the solid matrix due to deformation, and $\vec{v}_{i,s}$ is the velocity of phase i relative to the solid matrix, due to the pressure p_i in the phase, and is given by Darcy's law:

$$v_{i,s} = -\frac{k_{in,i}k_{r,i}}{\mu_i}\nabla p_i \quad i = w, g \tag{16}$$

Evaporation and condensation For phase change $\dot{I}$, a non-equilibrium formulation is used (Le et al., 1995; Scarpa and Milano, 2002; Halder et al., 2007) in which the volumetrically distributed evaporation/condensation is proportional to the difference between the equilibrium vapor density and the density of vapor in pores:

$$\dot{I} = K_{evap}(p_{v,eq} - p_v)\frac{S_g\phi}{RT} \tag{17}$$

where $p_v = p_g\omega_v$ is the vapor pressure, $p_{v,eq}$ is the equilibrium vapor pressure, and K_{evap} is the empirical evaporation constant, obtained from simulation studies (Halder et al., 2007; Gulati and Datta, 2016). Here $\dot{I}$ is positive for evaporation and negative for condensation. The phase change of butter is not considered in this study.

Table 2
Changes in input parameter.

Batter composition	M_0	T_{gel}	Source
Control	0.434	80 °C–90 °C	This study
+20% milk	0.473	80 °C–90 °C	This study
−20% milk	0.394	80 °C–90 °C	This study
+20% sugar	0.405	90 °C–100 °C	This study
−20% sugar	0.467	70 °C–80 °C	This study
+20% fat	0.415	90 °C–100 °C	This study
−20% fat	0.454	70 °C–80 °C	This study

Carbon dioxide generation For carbon dioxide generated from the double-acting baking powder, a zeroth order reaction having temperature dependency is used (Brodie and Godber, 2000; Godefroidt et al., 2019; Seranthian and Datta, 2023) with additional details provided in Seranthian and Datta (2023):

$$\dot{R}_{CO_2} = \begin{cases} \rho_s(1-\phi)(5\times10^{-4}(T-273.15) - 9.98\times10^{-5}), & T < 60\ °C \\ \rho_s(1-\phi)(5\times10^{-4}(313.15-273.15) - 9.98\times10^{-5}), & T \geq 60\ °C \end{cases} \tag{18}$$

Here $\dot{R}_{CO_2}$ is the mass generation rate of CO_2 in $kgCO_2/s$/volume of batter.

2.2.2. Large strain viscoelastic deformation

The governing equations for large-strain viscoelastic deformation are based on the conservation of linear momentum (Dhall and Datta, 2011) with additional details provided in Seranthian and Datta (2023):

$$\overline{\nabla}\cdot\overline{\sigma}_{eff} = \overline{\nabla}p_g \tag{19}$$

$$\overline{\sigma}_{eff} = J^{-1}\mathbf{F}\cdot\mathbf{S}\cdot\mathbf{F}^{\mathbf{T}} \tag{20}$$

where $\overline{\sigma}_{eff}$ is the effective stress at equilibrium and p_g is the gas pressure. The Lagrangian formulation for effective stress is related to J, the Jacobian, $\mathbf{F}$, the deformation gradient tensor, and $\mathbf{S}$, the second Piola–Kirchhoff (PK2) stress tensor. The solid velocity of the deforming porous matrix estimated by solving Eq. (19) is given by:

$$\overline{v_s} = \frac{d\overline{u}}{dt} \tag{21}$$

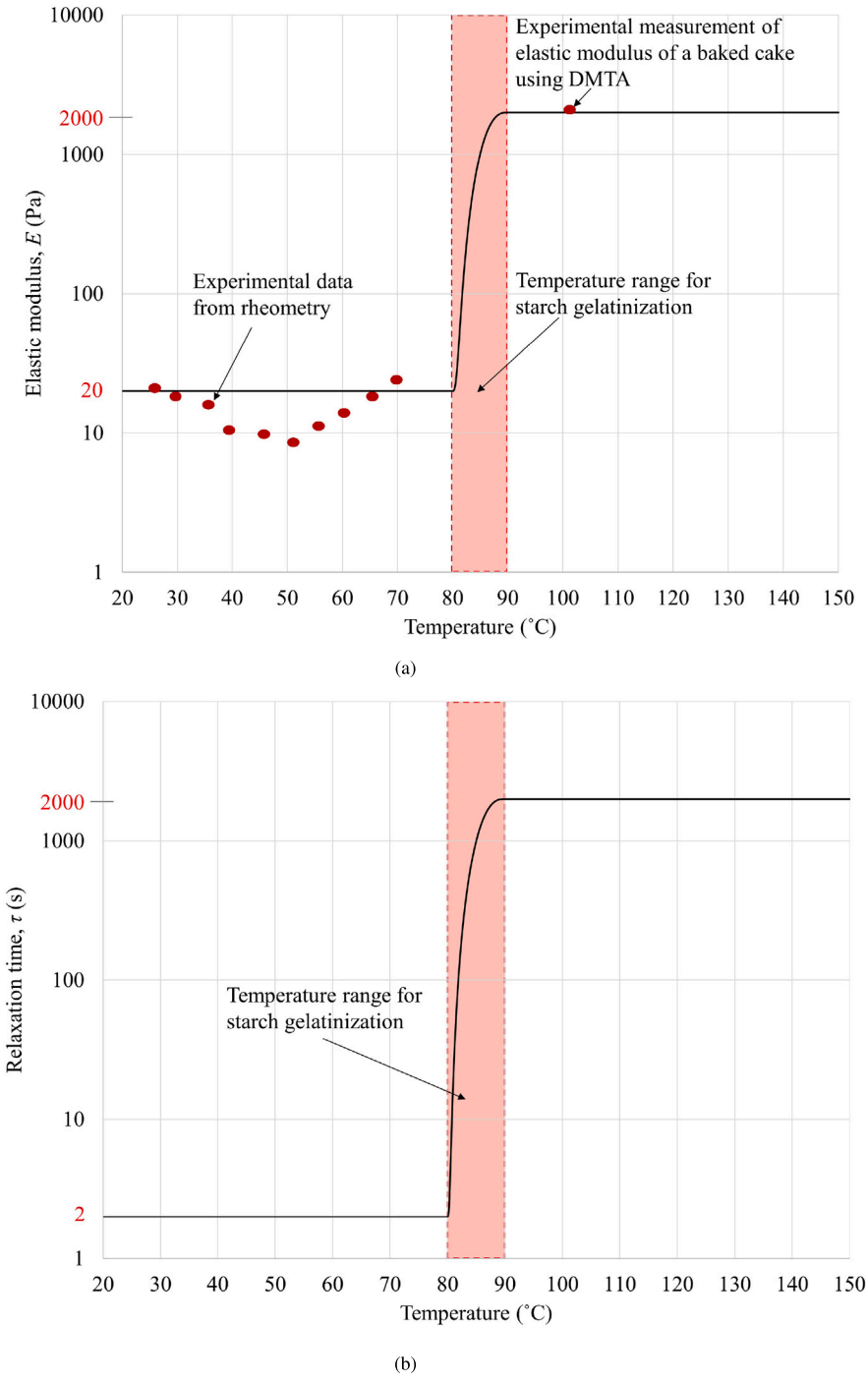

Fig. 4. The temperature-dependent evolution of (a) elastic modulus and (b) relaxation time.

The change in local porosity, ϕ, is estimated by the conservation of solid volume:

$$\phi(t) = 1 - \frac{(1-\phi_0)}{J} \tag{22}$$

2.2.3. Solid mechanics formulation: Constitutive law

Cake batters exhibit temperature-dependent viscoelasticity (Mizukoshi et al., 1979, 1980; Mizukoshi, 1985; Sumnu and Sahin, 2008; Seranthian and Datta, 2023). The linear first-order differential constitutive equation for viscoelasticity is given by:

$$\sigma(t) = E\varepsilon + \eta\dot{\varepsilon} \tag{23}$$

$$\varepsilon(t) = \frac{\sigma_0}{E}(1 - e^{-t/\tau}) \tag{24}$$

where ε, $\dot{\varepsilon}$ and σ_0 are the elastic strain, strain rate and instantaneous stress, respectively. $\tau = \eta/E$ is the relaxation time. The temperature dependence of modulus of elasticity, $(E(T))$ and relaxation time, $(\tau(T))$, capture temperature-dependent viscoelasticity.

2.3. Color model

The browning of cakes (yellow-gold color formation) is attributed to the Maillard reaction and caramelization of sugars (Zanoni et al., 1995; Fennema, 1996; Martins et al., 2000). The degree of surface browning can be quantified using the color difference, ΔE, measured at different times during baking, also referred to as Browning Index. It is calculated

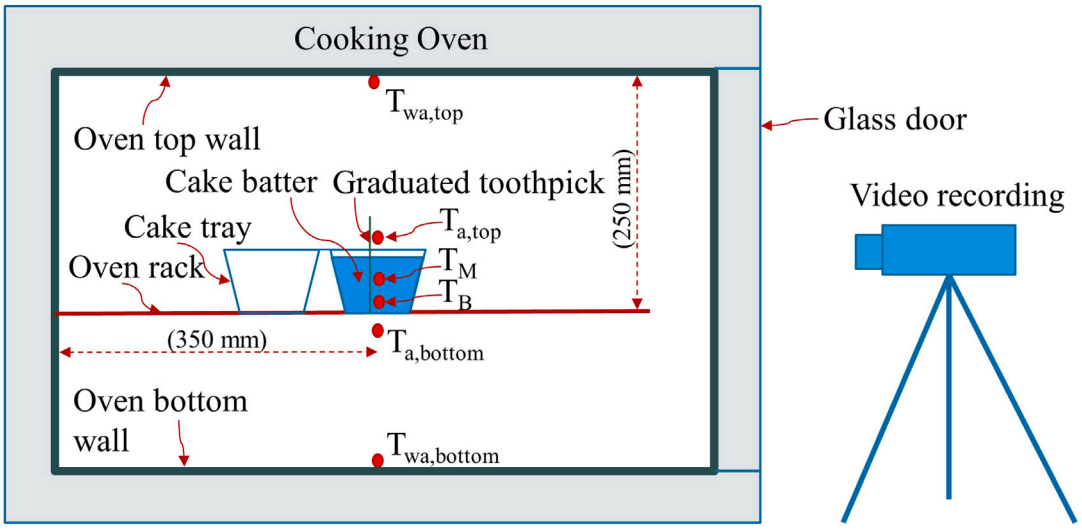

Fig. 5. Experimental setup showing temperature measuring locations, graduated toothpick for measuring oven rise, and video camera recording oven rise evolution with time. The cupcake is baked at the center of the oven cavity.

Table 3
Composition of raw (unbaked) batter for this study. The quantities in bold represent the change from the control recipe. The water content in butter is ignored in this study.

Ingredient	Control wt (g)	High water wt (g)	Low water wt (g)	High sugar wt (g)	Low sugar wt (g)	High fat wt (g)	Low fat wt (g)
Flour (12% water)	345	345	345	345	345	345	345
Sugar	350	350	350	**420**	**280**	350	350
Butter	226	226	226	226	226	**271.2**	**180.8**
Eggs (75% water)	240	240	240	240	240	240	240
Baking powder	12	12	12	12	12	12	12
Milk (87% water)	240	**288**	**192**	240	240	240	240
Salt	1.1	1.1	1.1	1.1	1.1	1.1	1.1
Vanilla extract	8.2	8.2	8.2	8.2	8.2	8.2	8.2
Moisture (kg water/kg solid)	0.43	0.47	0.39	0.41	0.47	0.41	0.45

Table 4
List of ingredients and brand name for cupcake baking experiments.

Ingredient	Make
Unbleached all purpose flour	Pillsbury
Granulated sugar	Domino
Unsalted Butter	Land O Lakes
Large white eggs	Eggland's Best
Baking powder	Clabber Girl
Whole Milk	Wegmans
Iodized salt	Morton
Vanilla extract	McCormick

based on the lightness (L^*), redness (a^*), and yellowness (b^*) values of the color:

$$\Delta E = \sqrt{(L_0^* - L^*)^2 + (a_0^* - a^*)^2 + (b_0^* - b^*)^2} \tag{25}$$

The browning reaction is temperature-dependent and follows first-order kinetics (Zanoni et al., 1995; Purlis and Salvadori, 2009):

$$\frac{d(\Delta E)}{dt} = -k_{br}(\Delta E) \tag{26}$$

$$k_{br} = k_0 e^{-A/T(t)} \tag{27}$$

where k_{br} represents the rate constant for browning. The parameters k_0 and A are fitting parameters, and $T(t)$ denotes the average surface temperature obtained from the computational model.

2.4. Boundary conditions

The boundary conditions for the governing equations, discussed in Section 2.2 and illustrated in Fig. 2, are presented below.

2.4.1. Multiphase transport

Boundaries 2, 3, and 4 receive convective and radiative heat. Boundaries 2 and 3 receive the same heat (the resistance of the metal tray is ignored).

$$\left.\frac{dT}{dr}\right|_{r=0} = 0 \tag{28}$$

$$q|_{2,3} = h_c(T_{a,bottom} - T) + h_r(T_{wa,bottom} - T) \tag{29}$$

$$q|_4 = h_c(T_{a,top} - T) + h_r(T_{wa,top} - T) - \lambda\, \vec{n}_{w,s}\big|_4 - \sum_{i=w,v,\mathrm{CO_2}} (\vec{n}_{i,G}\big|_4) C_{p,v} T \cdot \vec{N}\Big|_4 \tag{30}$$

where q is the inward heat flux. $T_{a,bottom}$ and $T_{a,top}$ are the measured air temperatures below and above the cupcake tray, $T_{wa,bottom}$ and $T_{wa,top}$ are the temperatures of the oven bottom and top wall, and h_c and h_r are the heat transfer coefficients for convective and radiative heat exchange, respectively. The boundary conditions for radiative heat exchange, $h_r(T_{wa,bottom} - T)$ and $h_r(T_{wa,top} - T)$, are linearization for computing efficiency of $\sigma F_{wa,bottom-surf}(T^4_{wa,bottom} - T^4)$ and $\sigma F_{wa,top-surf}(T^4_{wa,top} - T^4)$ respectively (Incropera and DeWitt, 1985), where σ is the Stefan–Boltzmann constant, and $F_{wa,top-surf}$ and $F_{wa,bottom-surf}$ are the view factors between the wall and cake surfaces. It is assumed that surface 4 sees only the top wall and surfaces 2 and 3 see only the bottom

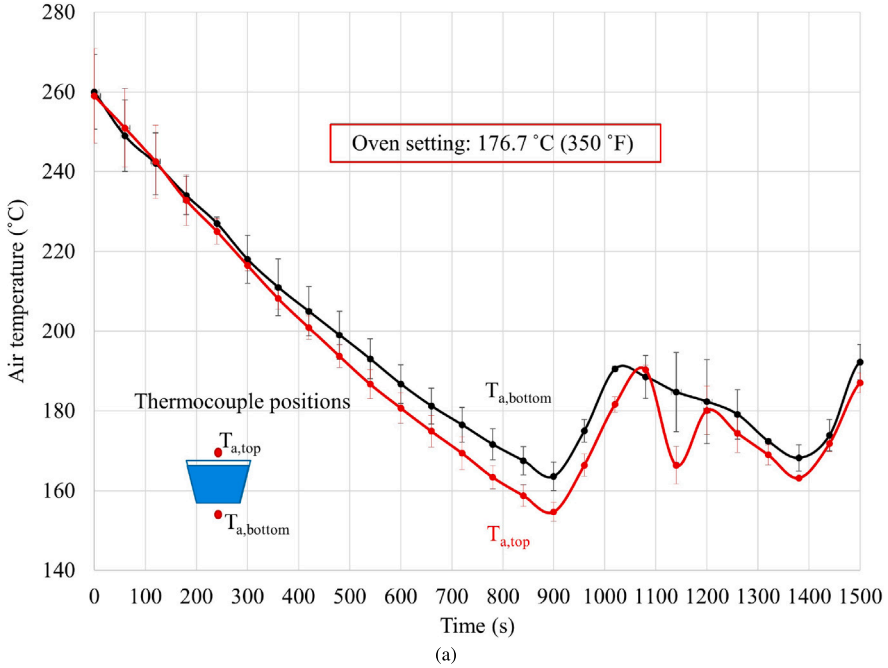

Fig. 6. (a) Measured air temperatures inside the oven above and below the cupcake tray and (b) wall temperatures inside the oven during baking. The error bars represent variations observed between experiments.

wall for radiative exchange. The assumption for surface 3 simplifies the complexity of the radiative exchange and experimental measurements. Surface 3 exchanges radiation with the oven side, front, back and the adjacent cupcake tray surfaces, which is extremely complex. The bottom wall is the primary driver (see Fig. 6(b), which shows a much higher temperature), and the view factor between surface 3 and the bottom being significant, we set up the simplified radiative exchange using the radiative heat transfer coefficient and bottom wall temperature. The third and fourth terms in Eq. (30) represent evaporative and sensible heat loss from the cupcake surface. Experimental measurements of air and surface temperatures are discussed in Section 4.2.

Boundaries 1, 2, and 3 have zero mass flux boundary conditions. Boundary 4 has a convective mass transfer boundary condition and accounts for solid surface deformation with an additional flux. For the gas transport equation (Eq. (3)), Boundary 4 is set to the ambient pressure condition:

$$\vec{n}_{w,G}|_4 = h_m S_w \phi \rho_{g,4} \omega_{v,4} + c_w \vec{v}_s \tag{31}$$

$$\vec{n}_{v,G}|_4 = h_m S_g \phi \rho_{g,4} \omega_{v,4} + c_w \vec{v}_s \tag{32}$$

$$p|_4 = p|_{amb} \tag{33}$$

2.4.2. Large strain viscoelastic deformation

Eq. (19) calculates the deformation ($\vec{v}_s$) of the cake batter during baking. Boundary 1 (axis of symmetry) and boundary 3 (lateral surface)

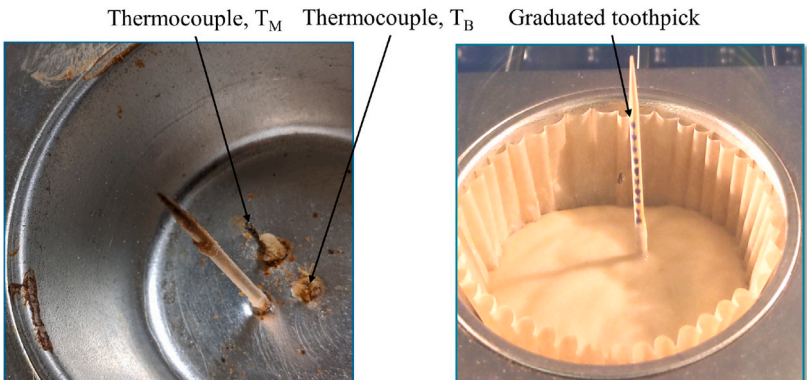

Fig. 7. Experimental setup for measuring (a) the cupcake's internal temperature and (b) its oven rise. The cupcake thermocouples are 2 mm and 11 mm from the bottom surface of the cupcake tray. The toothpick and the thermocouples are fixed at a radial distance of 2 mm from the center of the tray.

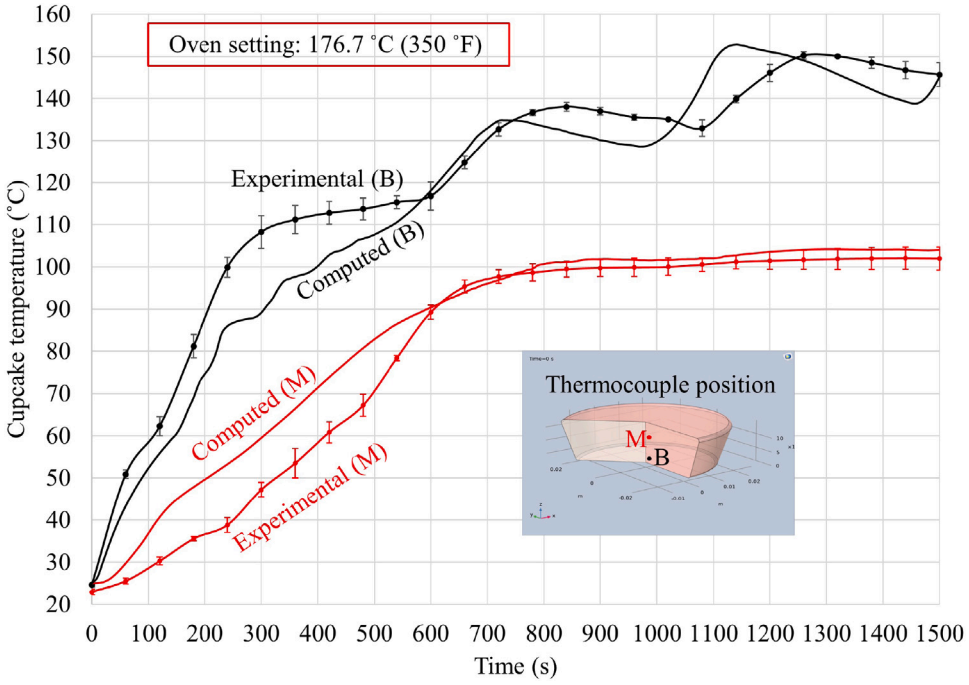

Fig. 8. Cupcake temperatures close to the center (M) and close to the bottom surface (B) with the oven set at 176.7 °C (350 °F).

have zero normal displacement boundary conditions (the model computes tangential displacement). Boundary 2 (bottom surface) is fixed, while boundary 4 (top surface) is unconstrained.

2.5. Input parameters

Table 1 provides a summary of the input parameters used to simulate baking the control recipe. Important details regarding certain key parameters are outlined below.

2.5.1. Permeability

Fig. 3 shows the temperature-dependent intrinsic permeability of liquid water through the cake batter undergoing massive changes in its material state. The high permeability batter is characterized by a constant permeability value of 1×10^{-10} m^2, which decreases to 5×10^{-13} m^2 for the low permeability solid cake after starch gelatinization (Lostie et al., 2004). The permeability change is assumed to coincide with the material transformation of the batter from an almost liquid to a solid foam at the starch gelatinization temperature. This is because, in preliminary studies and from literature (Zhang and Datta, 2006), it is found that large permeability causes no appreciable pressure buildup inside the batter to cause deformation because the generated vapor bubbles out of the liquid batter easily. The solid foam formed after material transformation at the starch gelatinization temperature is less permeable than the runny (almost liquid) batter, giving more resistance to mass transfer.

2.5.2. Water activity

Due to the lack of available water activity data for baking, this study uses Oswin's empirical relation (Basu et al., 2006; Andrade et al., 2011), fitted to the desorption isotherm specific to sponge cake batter (Lostie et al., 2002) as previously demonstrated for dough baking by Nicolas et al. (2016) with additional details provided in Seranthian and Datta (2023).

$$\begin{aligned} 100M &= A\left(\frac{a_w}{0.65-a_w}\right)^B \\ with &\begin{cases} A = 15.64 - 0.1(T-273.15) \\ B = 0.38 + 1.69\times10^{-3}(T-273.15) \end{cases}, T < 373.15\ \text{K} \\ 100M &= A\left(\frac{a_w}{0.65-a_w}\right)^B \\ with &\begin{cases} A = 15.64 - 0.1(373.15-273.15) \\ B = 0.38 + 1.69\times10^{-3}(373.15-273.15) \end{cases}, T \geq 373.15\ \text{K} \end{aligned} \tag{34}$$

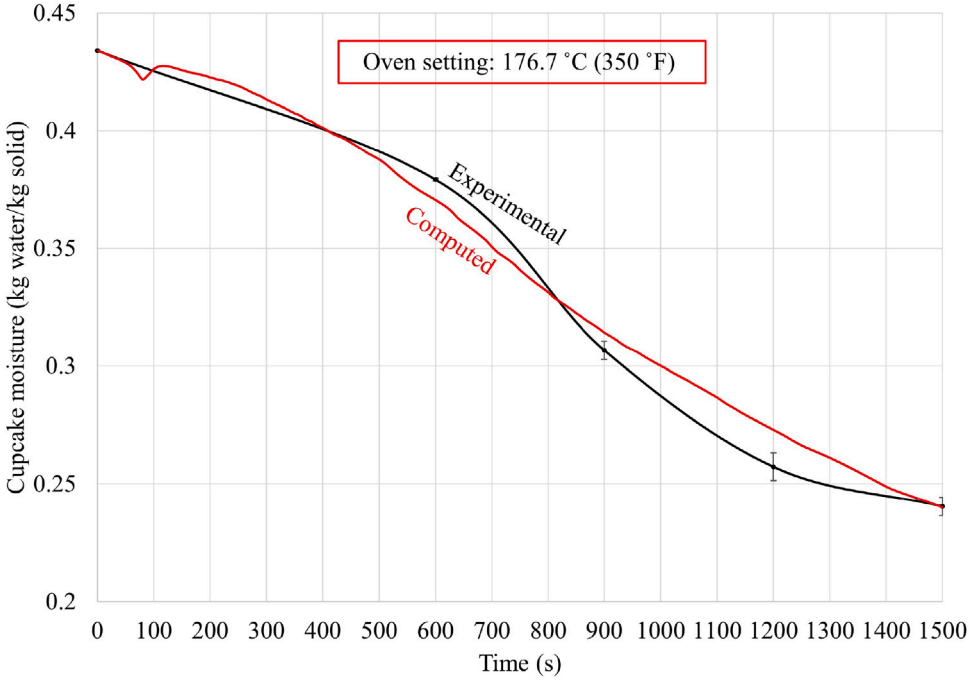

Fig. 9. Moisture content of the cupcake during baking with the oven set at 176.7 °C (350 °F).

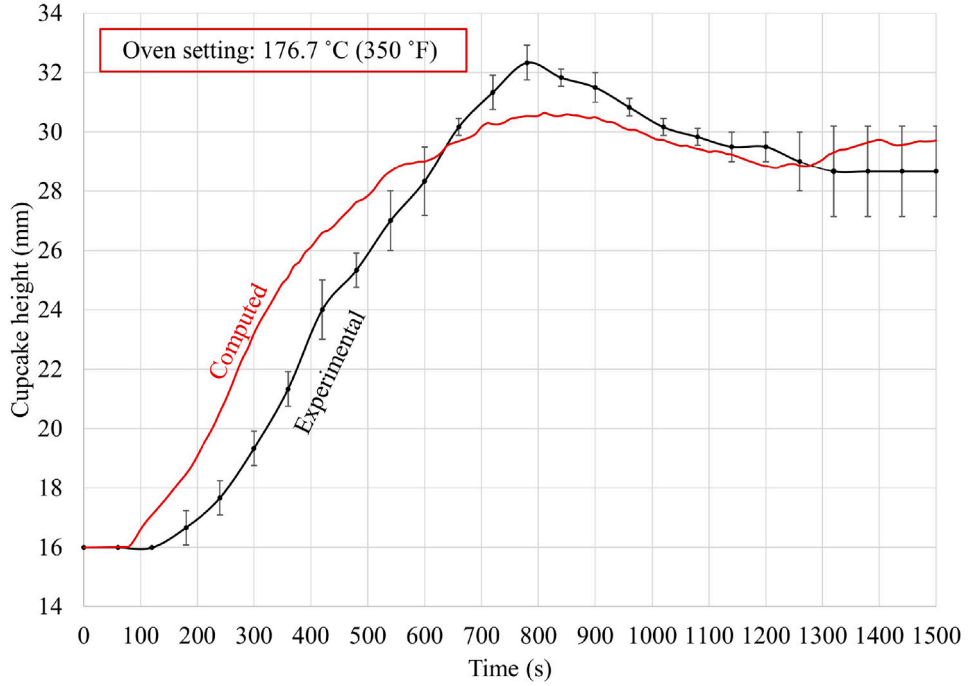

Fig. 10. Oven rise of the cupcake during baking in the oven set at 176.7 °C (350 °F).

2.5.3. Material modulus and relaxation times

Fig. 4(a) shows the temperature-dependent elastic modulus used in the study. The elastic modulus increases from 20 Pa to 2000 Pa as the material transitions from an almost liquid (rubbery state) to a solid foam (glassy state) with increasing temperature, as observed through rheometry and Dynamic Mechanical Thermal Analysis (DMTA) data (Guy and Sahi, 2006). For the temperature-dependent relaxation time (Fig. 4(b)), a short relaxation time of 2 s is assumed for the liquid batter (Zhang and Datta, 2006; Nicolas et al., 2016), followed by an increased relaxation time of 2000 s for the set solid foam after starch gelatinization occurs between 80 °C to 90 °C (Godefroidt et al., 2019).

2.5.4. Ingredient functionality

Most input parameters for the different recipes in this study are unavailable in the literature. Measuring them from scratch was beyond the scope of this study due to constraints on time and resources. Changing water content will likely impact rheology, and changing sugar content will likely affect water activity (Pyler and Gorton, 2008). Getting experimental temperature-dependent rheological and water activity data for

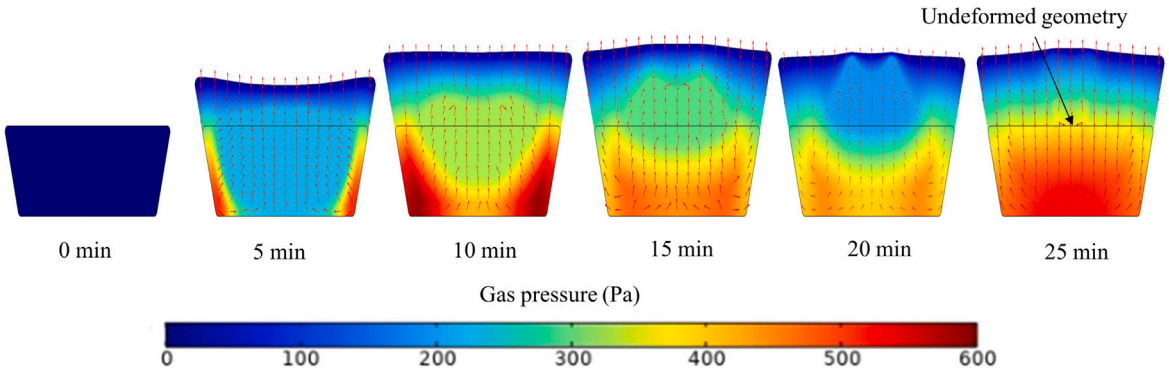

Fig. 11. Gas pressure (gauge pressure) evolution inside the cupcake during baking.

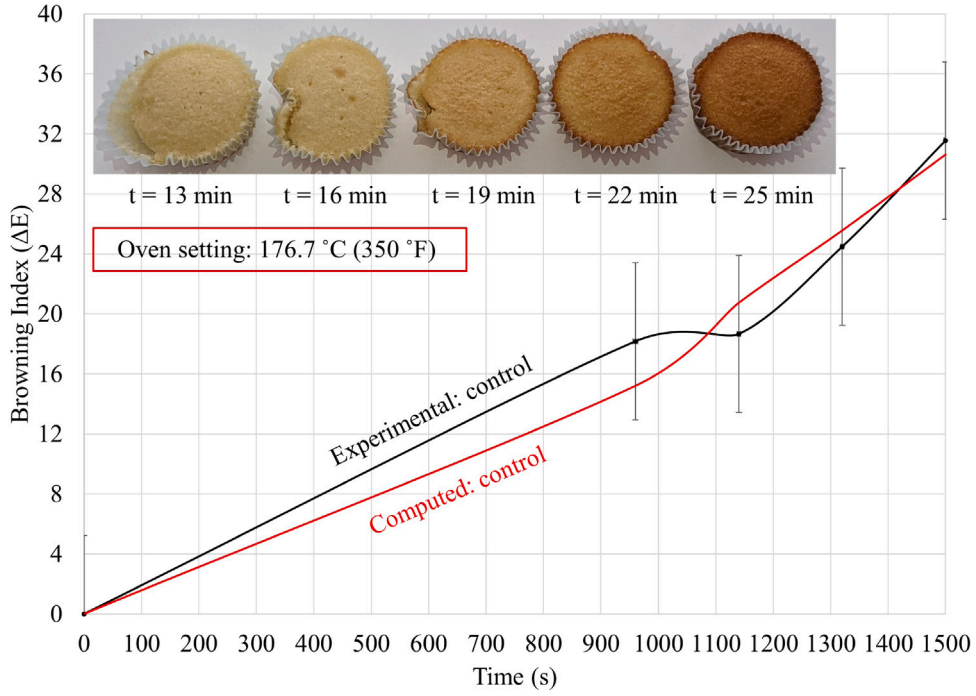

Fig. 12. Surface browning of the cupcakes during baking in the oven set at 176.7 °C (350 °F).

all seven batter recipes was not possible. Hence, only two parameters are varied in this study. A sensitivity analysis of rheology and water activity for a similar recipe is provided in Seranthian and Datta (2023). Table 2 summarizes the changes to input parameters used in simulating ingredient functionality in the cake baking process. The model parameters defining material transformation at the starch gelatinization temperature, T_{gel}, are temperature-dependent intrinsic permeability, elastic modulus, and relaxation time (Guy and Sahi, 2006; Lostie et al., 2004; Zhang and Datta, 2006; Nicolas et al., 2016; Godefroidt et al., 2019). For cake batters, which are complex polymeric emulsions, the starch gelatinization temperature, T_{gel}, is typically measured using the 'not so accurate' Rapid Visco Analyser (RVA) and are not available for the exact recipes. Due to the lack of measured starch gelatinization temperatures for the different recipes used, the study uses the gelatinization temperatures for similar sugar-flour ratios from Bean and WT (1978). Sugar raises starch gelatinization temperature by limiting water availability to starch (Bean and WT, 1978; Beleia et al., 1996; Spies and RC, 1982; Pyler and Gorton, 2008). There still needs to be more research regarding the effects of fat addition and types of fat on starch gelatinization. Fat melts and coats ingredients (waterproof), limiting the immediate hydration of starch in the batter during baking, having a very similar effect as sugar on starch gelatinization (Eliasson, 1985; Putseys et al., 2010; Arik Kibar et al., 2014). Based on this, the impact of fat on gelatinization temperatures is assumed to follow the same trend as sugar, given the unavailability of data for the chosen recipes.

2.5.5. Color kinetic parameters

The fit parameters in Eq. (27) were estimated by minimizing the sum of squared differences between the average experimental and predicted browning indices of the cupcakes. The lsqnonlin solver in MATLAB (R2017a, The Mathworks Inc., MA, USA) was used for nonlinear least squares optimization. The average surface temperature of the control recipe cupcake, computed by the model, was used for the parameter estimation. The kinetic parameters were used to validate the experimental browning data for cupcakes baked with recipes different from the control recipe.

3. Computational methodology

A 2D axisymmetric computational domain with a triangular mesh comprising 11,374 elements was used to study the multiphase transport and large strain viscoelastic deformation in the baking process.

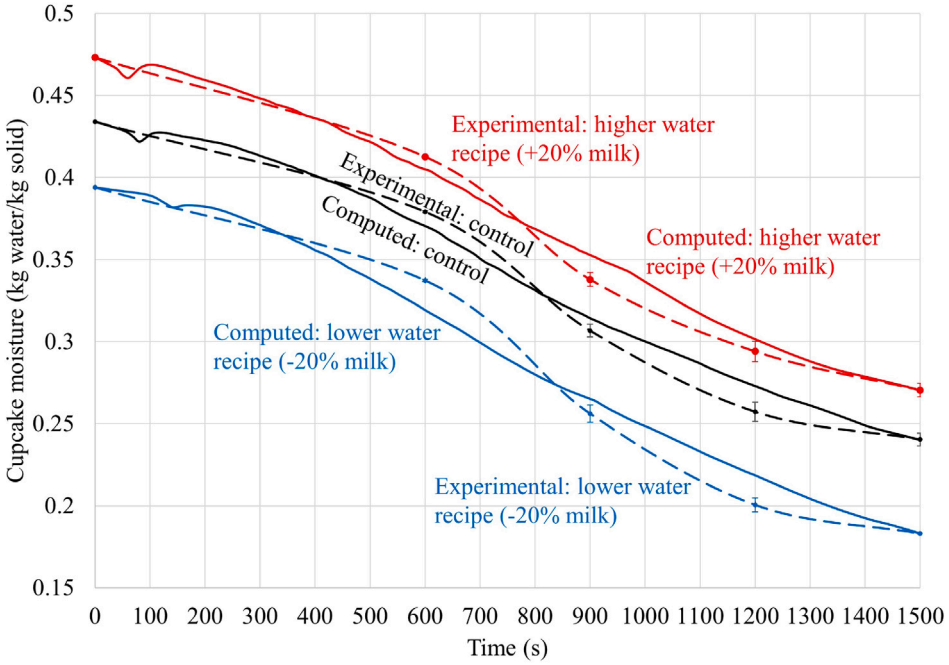

Fig. 13. Moisture content of the cupcake during baking for batters of different initial water contents.

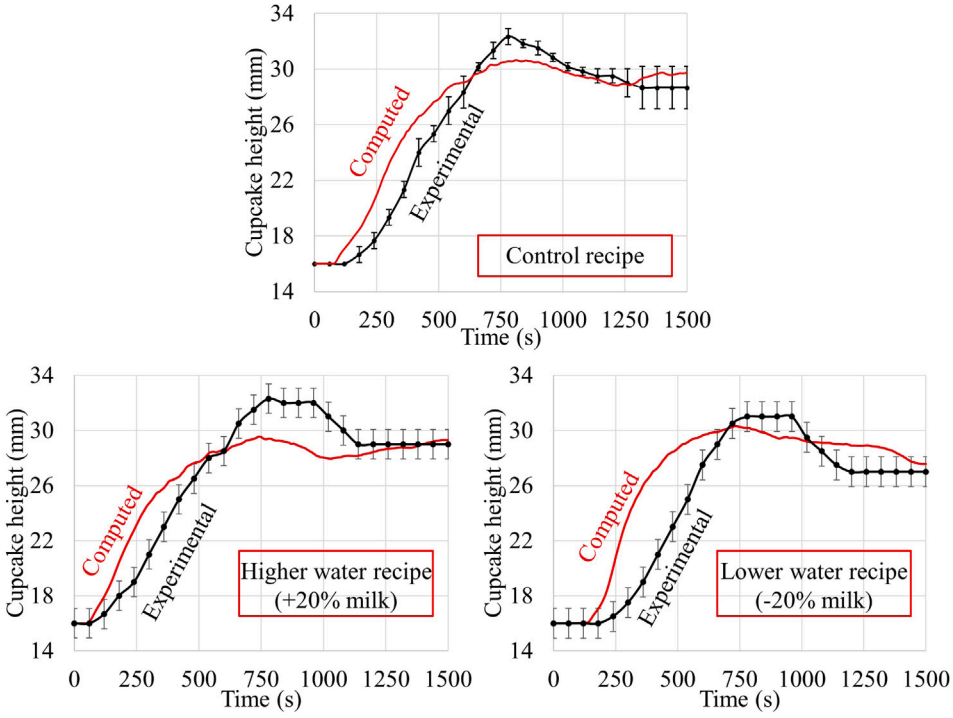

Fig. 14. Oven rise of the cupcakes during baking for batters of different initial water contents.

More details of the computational methods are provided in detail in Seranthian and Datta (2023).

4. Experimental methodology

4.1. Baking experiments

Cupcakes with various compositions (as listed in Tables 3 and 4) were baked for 25 min in a Whirlpool gas oven (model: WFG530S0EW) with a capacity of 1.4×10^{-1} m^3 (5 cubic ft). The oven was preheated to 176.7 °C (350 °F). Fresh cake batter was prepared for each experiment using a stand mixer (KitchenAid, Artisan Series 5) set to speed 4. The butter and sugar were mixed for 2 min, followed by the addition of presifted flour, salt, baking powder, vanilla extract, milk, and eggs. The mixture was beaten at speed 4 for an additional 2 min. For each experiment, 28 grams of batter was placed in a cupcake baking tray lined with parchment paper and coated with Teflon. The cupcakes were baked using the setup illustrated in Fig. 5. Each experiment involved

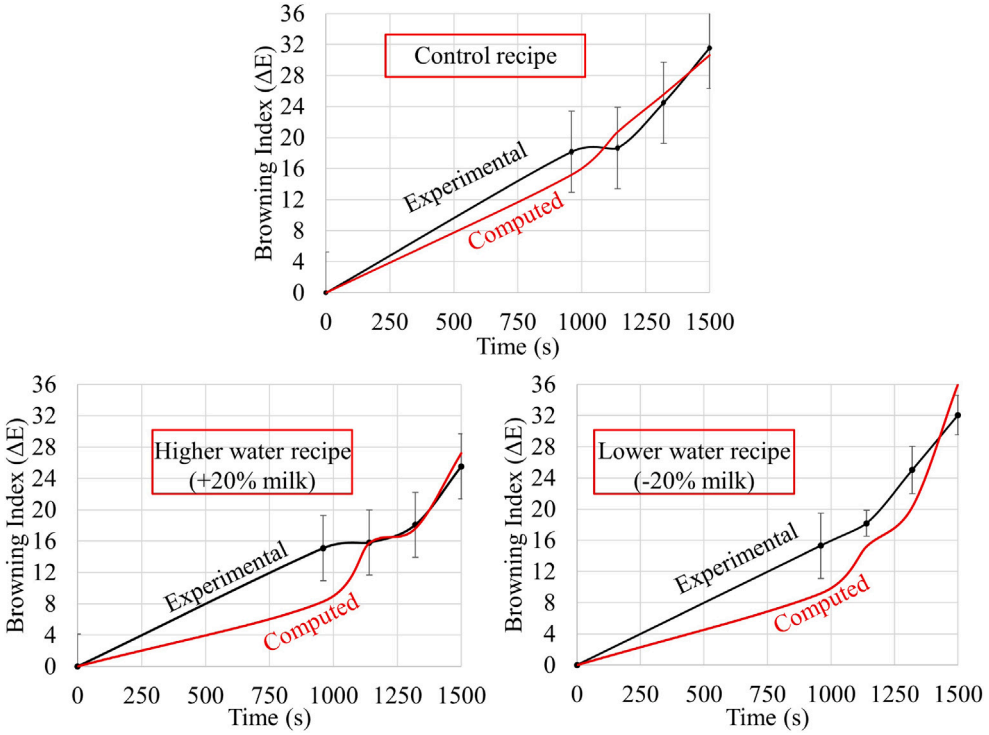

Fig. 15. Surface browning of the cupcake during baking for batters of different initial water contents.

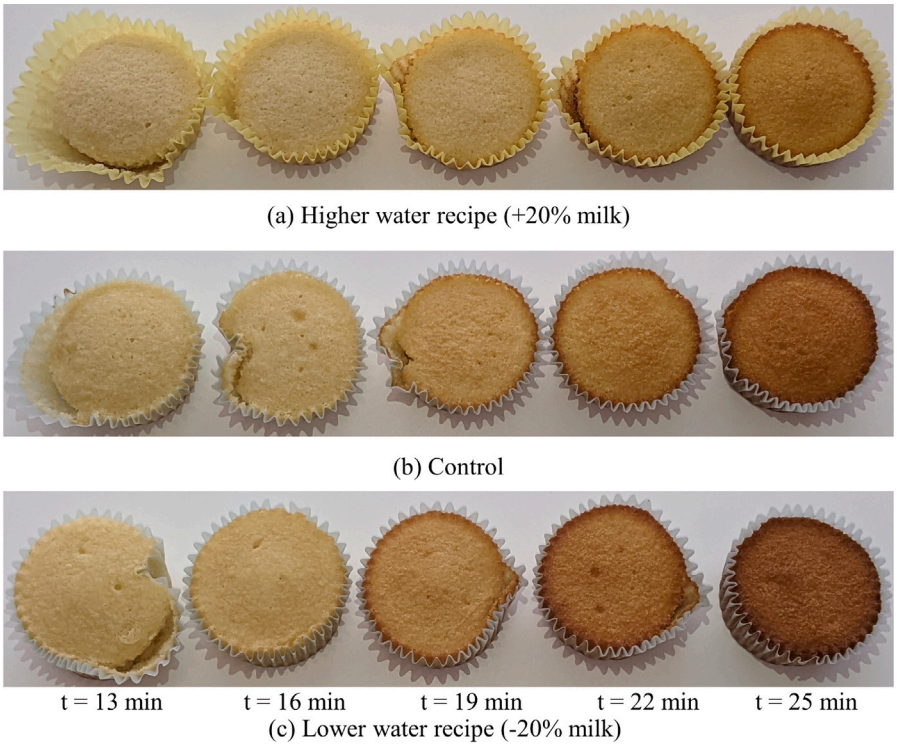

Fig. 16. Surface browning of the cupcake during baking for batters of different initial water contents.

baking a single cupcake from a fresh batter, after which the batter was discarded. Three replicates were conducted for each measurement with fresh batter. The variability among experiments is represented by error bars on the averaged quantities derived from all measurements in the experiments. The experiments were repeated with different recipes.

4.2. Air and wall temperature measurement

Air temperatures ($T_{a,top}$, $T_{a,bottom}$), above and below the cupcake tray, were measured by thermocouples ($T_{a,top}$, $T_{a,bottom}$), fitted 10 mm above and below the cupcake tray (Fig. 5), respectively. Top and bottom

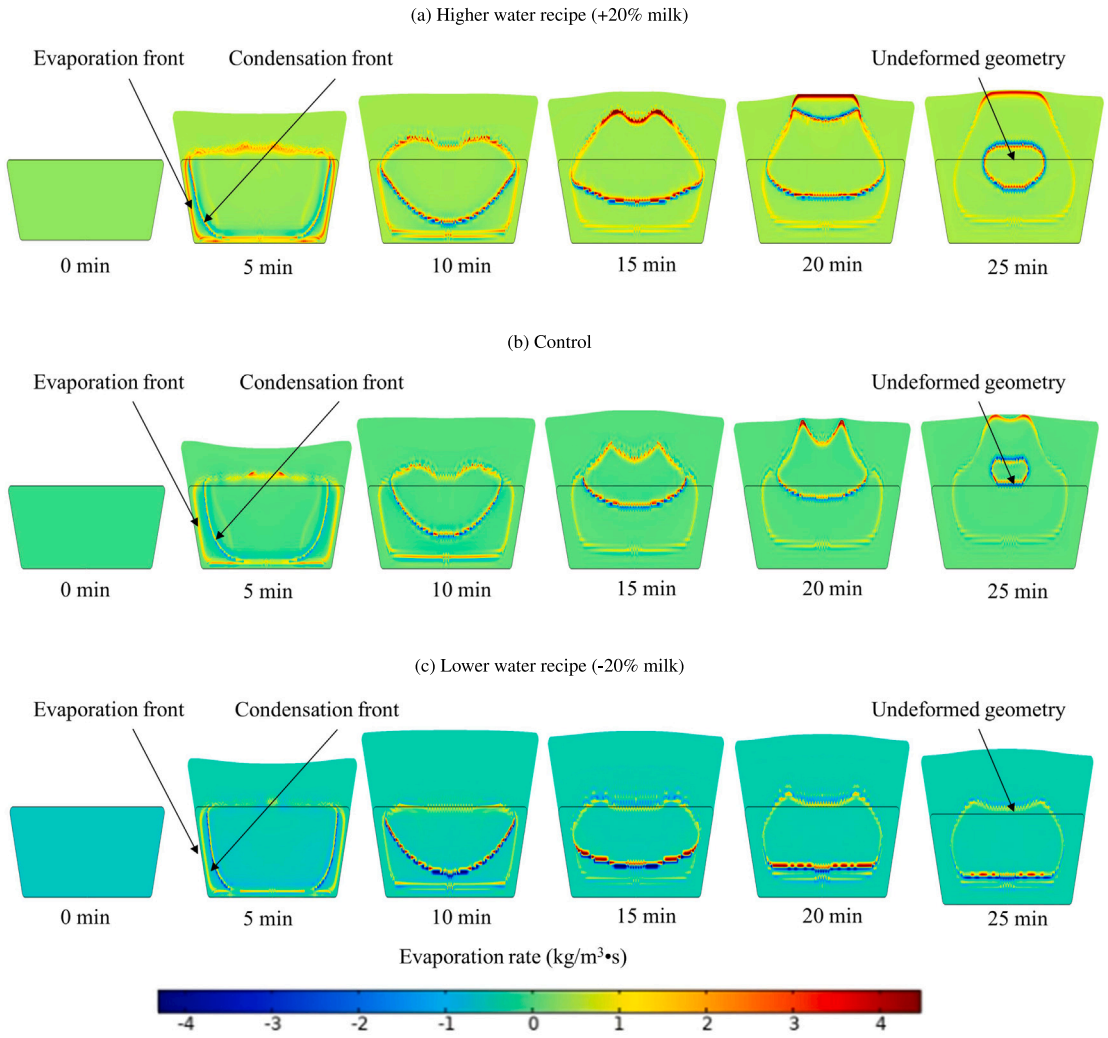

Fig. 17. Evaporation rate profiles inside the cupcake during baking for batters of different initial water contents, showing higher evaporation for higher water content recipe.

wall temperatures, $T_{wa,top}$ and $T_{wa,bottom}$, also measured using the same type of thermocouples, were taped on the respective walls of the oven cavity (Fig. 5), respectively. Omega Engineering Inc. K-type (accurate to ±2.2 °C) thermocouples were used to measure air temperatures (Figs. 6(a),6(b)), which exhibited significant variations due to the oven duty cycle, as the heating elements turn on at different times following its own algorithm to maintain the set air temperature at the oven center. Air temperatures inside the oven can reach a very different (higher or lower than set) temperature at the end of preheating due to several reasons, including thermal leakages due to wear and tear, changes in wall emissivities due to food spillage, cleaning, and broken sensors as seen in Fig. 6(a).

4.3. Cake internal temperature and oven rise measurement

The cupcake's internal temperatures were measured by two thermocouples, one positioned 2 mm from the bottom surface and another placed at the center, 11 mm from the bottom (Fig. 7). The cupcake's height (approximately at the center) throughout baking was recorded using a calibrated toothpick fixed at 2 mm from the center (Fig. 7).

4.4. Moisture loss and color measurement

The moisture loss during baking was determined by weighing the cupcakes at specific time intervals: 10, 15, 20, and 25 min. A digital kitchen scale with an accuracy of +/− 0.1 grams was used to measure the weight loss, which is assumed to be due to moisture loss. After weighing, the cupcakes were discarded, and the experiment was repeated for subsequent baking durations using fresh batter.

The color properties of the cupcake's top surface, lightness (L^*), redness (a^*), and yellowness (b^*), were measured using a VeyKolor colorimeter (Hangzhou Baiteng Electronic Technology Co., Ltd., Zhejiang, China) (accurate to $\pm 0.08\Delta E$) under white light (75 Watt LED bulb, 1100 lumens) after being weighed at time intervals: 15, 20, and 25 min. Browning Indices (ΔE) were computed from the recorded L^*, a^*, and b^* values (Eq. (25)).

4.5. Mechanical properties measurement

The temperature-dependent elastic modulus of the cupcake batter was determined using an oscillatory shear test. One milliliter of freshly prepared cupcake batter was placed between 40 mm parallel plates, and a temperature sweep was conducted from 25 °C to 70 °C at a frequency of 0.1 Hz. The measurements were performed using a calibrated TA Instruments Discovery Hybrid HR-3 rheometer. For baked cupcakes, a compression test was carried out on cubic samples measuring 10 mm × 10 mm × 10 mm. These samples were cut out from freshly baked cupcakes. The compression test was conducted using a TA Instruments DMA Q800 Dynamic Mechanical Thermal Analysis instrument. Three replicates were performed, and the average moduli obtained from these replicates were recorded (Fig. 4(a)).

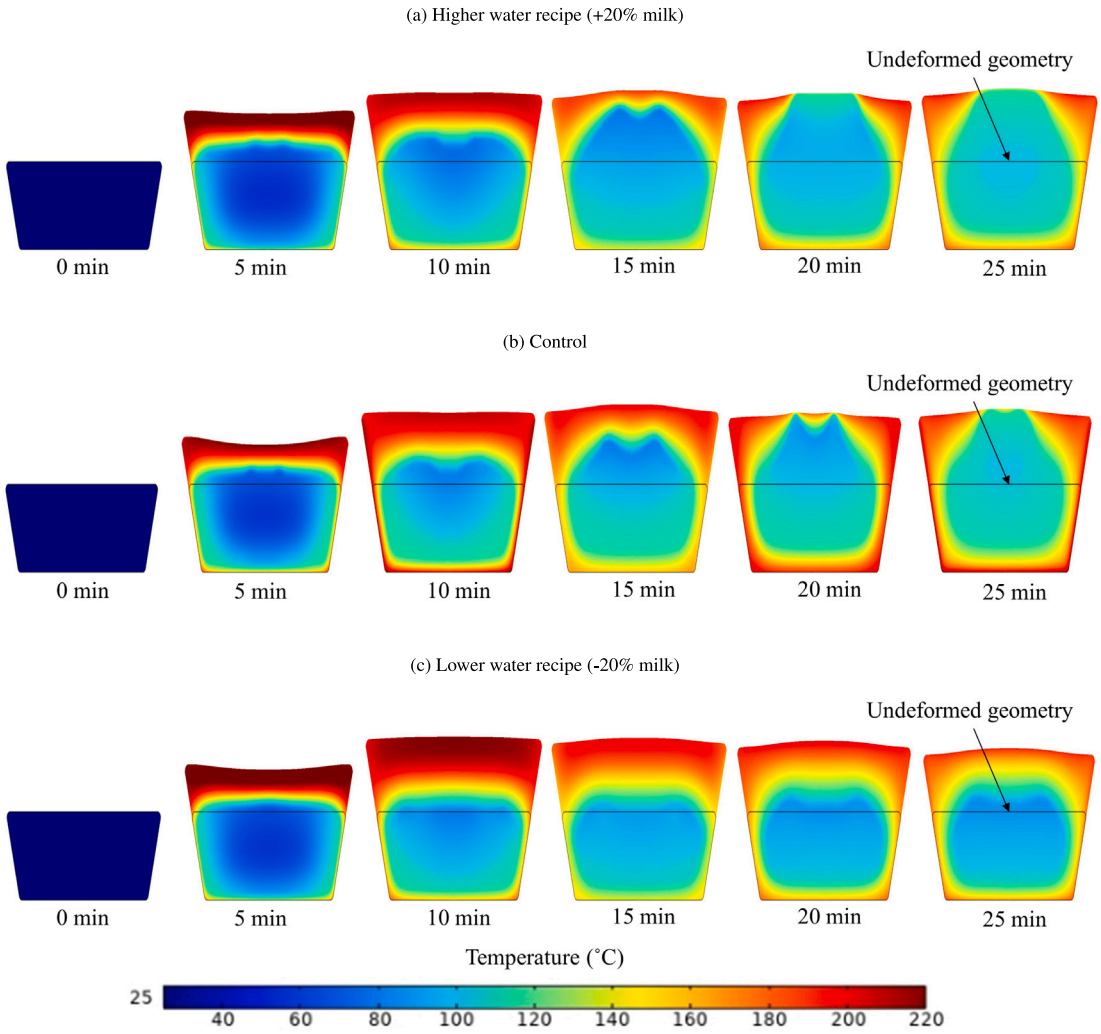

Fig. 18. Temperature profiles inside the cupcake during baking for batters of different initial moisture contents.

5. Results and discussions

The computational simulations were validated against experimental measurements of internal temperature, moisture loss, and oven rise data obtained during baking. After validation, the model was used to investigate the influence of ingredients on the model parameters and their impact on the cupcake's height, weight, and color during baking, utilizing both the simulations and the corresponding experimental results.

5.1. Experimental validation

Measured and predicted temperatures at two different points inside the cupcake during baking are compared in Fig. 8. The model predicts lower temperatures close to the bottom surface and higher temperatures close to the cupcake's center during the initial stage of baking. A better agreement with measured temperatures is seen after 600 s of baking. Previous attempts (Sakin et al., 2007) at fully mechanistic modeling of baking, including our work (Seranthian and Datta, 2023), have found it challenging to match temperatures during the initial stages of baking, perhaps due to the complexity during the initial stages arising from massive changes in mechanical properties as the batter transforms from high permeability liquid batter to low permeability solid foam. The significant variations in carefully replicated oven rise experiments also represent the process complexity. The temperature rise inside the cupcake shows two distinct phases, an initial steady rise and a subsequent stabilization phase. In the initial phase, the linear temperature rise indicates a combination of conduction, convection and evaporative heating, followed by a plateau representing an almost pseudo-steady state where the incoming heat from the boundary balances the large latent heat of evaporation in the cupcake body. The oven air and radiant temperatures that drive the baking process fluctuate (Figs. 6(a) and 6(b)), the effect of which is visible in the cupcake temperatures close to the bottom surface (location B). The geometric center does not see the impact of these fluctuating driving temperatures as it is deeper inside, and the significant evaporation in the cupcake body muffles the effect of surface variation deep inside.

Fig. 9 shows observed and predicted moisture loss from the entire cupcake during baking to be in excellent agreement. The effect of the oven's cyclic air and wall temperatures that drive the process is not clearly evident in the evolution of total moisture loss.

Measured and predicted oven rise of the cupcake during baking are compared in Fig. 10. The model predicts no initial oven rise for the first 80 s, followed by a significant increase of over 90% in size between 80 and 800 s. Subsequently, there is continuous shrinkage of approximately 10% until around 1250 s and a slight oven rise of about 5% for the remainder of the baking cycle. The implemented model agrees with the observed evolution of oven rise (Fig. 10). However, it slightly overestimates the oven rise between 80 and 600 s. The substantial variation in oven rise at different baking stages, driven by changes in gas pressure within the batter (Fig. 11), is attributed to the transformation of the batter's mechanical properties throughout baking.

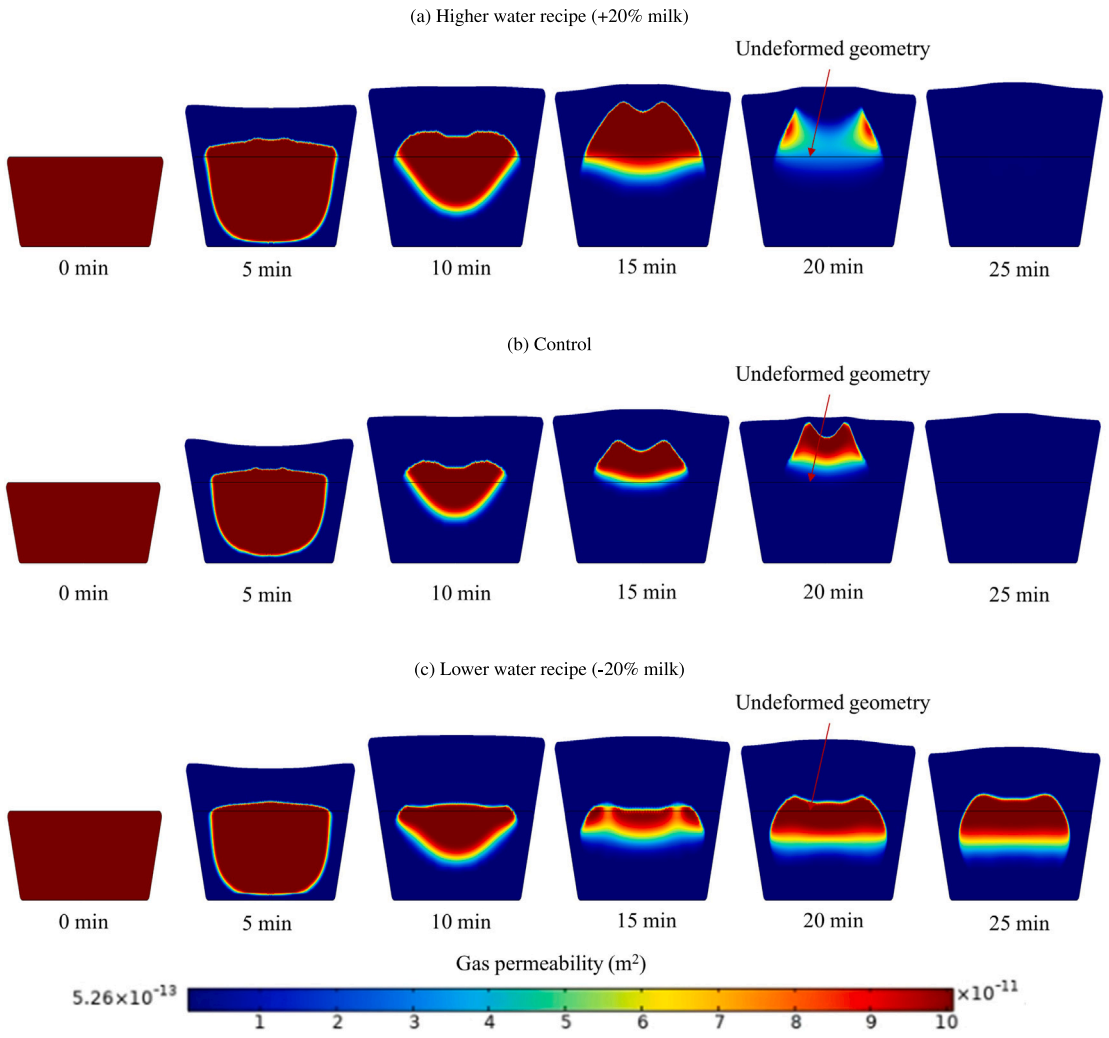

Fig. 19. Gas permeability inside the cupcake during baking for batters of different initial moisture contents (deep blue regions are solid foam and dark red are liquid batter).

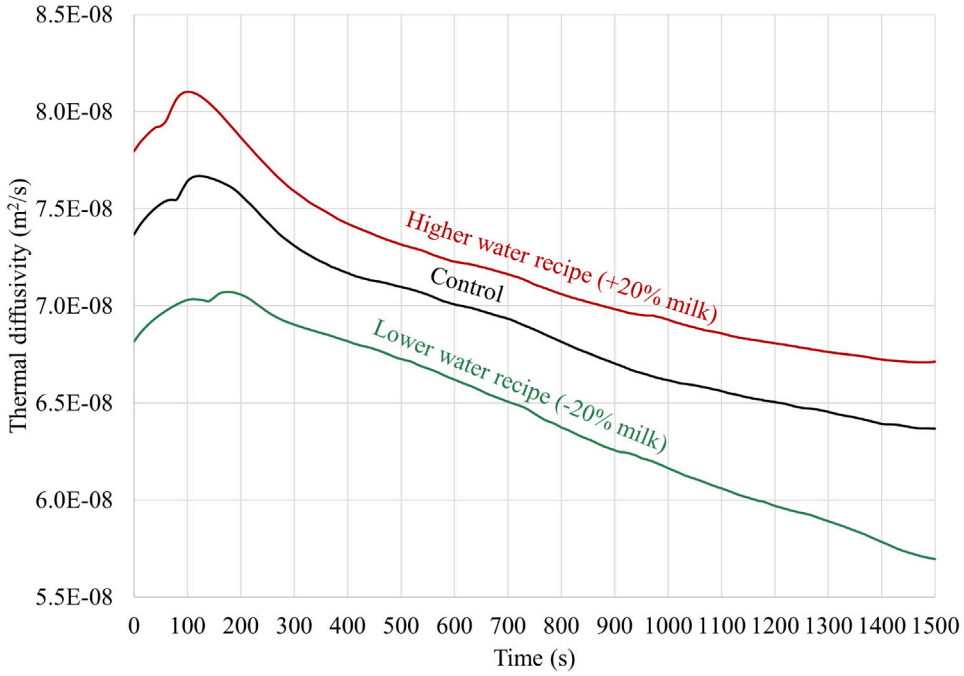

Fig. 20. Average thermal diffusivity (model predicted) of the cupcake during baking for batters of different initial water contents.

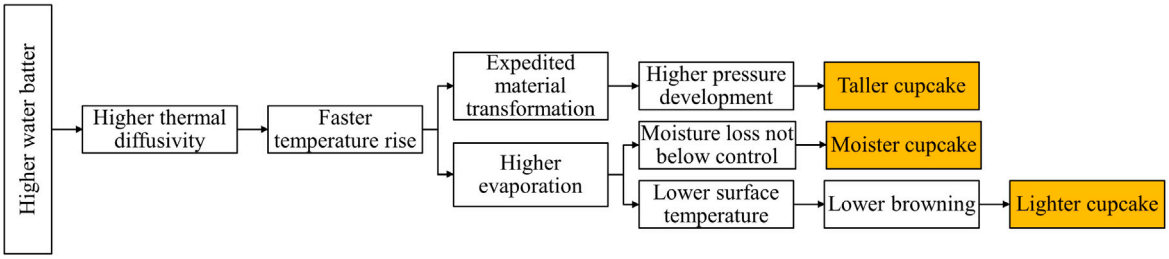

Fig. 21. Role of water on moisture loss, oven rise, and browning of cupcakes, summarizing the mechanistic understanding developed using model and experiments. The effect of water on oven rise is not obvious from experiments.

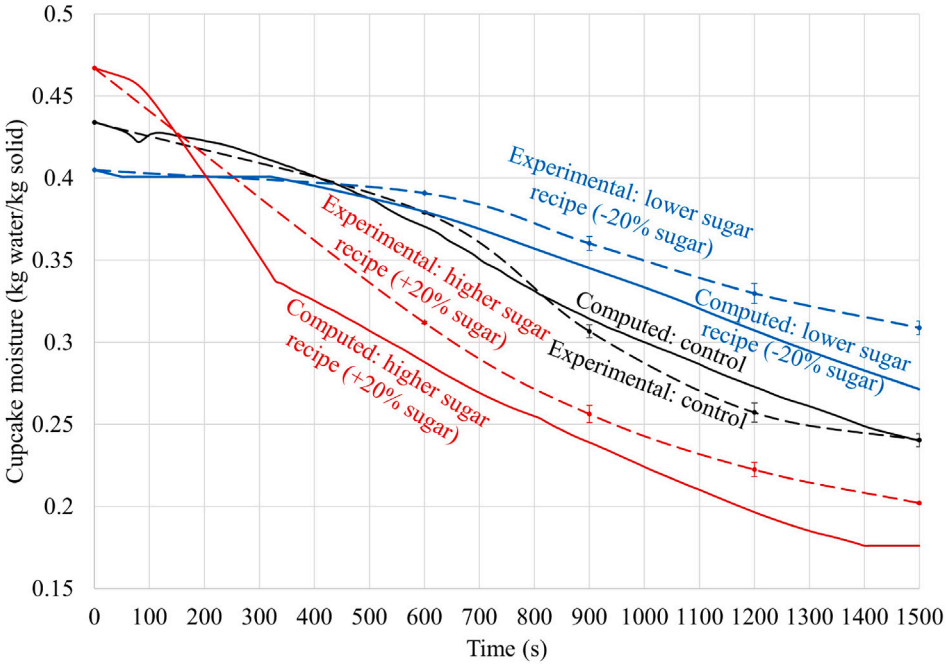

Fig. 22. Moisture content of the cupcakes during baking for batters of different sugar content.

In the early stages of baking, vapor and carbon dioxide generated in the batter diffuse out of the cupcake without contributing to pressure development (Fig. 11). As the liquid batter transitions into a less permeable solid from the outer region to the center, pressure builds up due to trapped gas (Fig. 11). Towards the end of baking, the oven rise diminishes due to the reduced water availability for vapor generation via evaporation. The quantitative discrepancy between experimental and predicted oven rise and the variations in measured oven rise from meticulously repeated experiments underscore the complexity of the underlying physics in the process and the associated challenges.

The empirical model for surface browning (Fig. 12) matches well with the experimental data. The model parameters (Eq. (27)) are computed by fitting the model predictions to the experimental surface browning for the control recipe baked in the oven set at 176.7 °C (350 °F). Initially, no visible browning is observed until approximately 16 min of baking. Significant variations between experiments highlight the complex nature of browning development.

5.2. Ingredient functionality

5.2.1. Role of water

Change in water content affects moisture loss, oven rise, and browning, as shown in simulations compared with experimental results (Figs. 13–16). Among the selected recipe variations, the batter with the highest initial moisture content (+20% milk), despite having higher evaporative loss throughout baking (Figs. 17(a)–17(c)), had more moisture at the end of baking compared to the batter with the lowest initial water content (−20% milk). The evaporation front (where vapor generation occurs) is stronger for the higher water recipe. The pressure developed during evaporation pushes the hot vapor towards the colder cupcake, causing condensation (condensation front). Due to higher pressures from increased evaporation, the condensation front is farther from the evaporation front for the higher water recipe. The higher water content batter has higher internal temperatures during baking (Figs. 18(a)–18(c)), likely due to higher effective thermal diffusivity (Fig. 20), leading to higher evaporation.

Fig. 14 shows oven rise (height change) during baking, as affected by water content, with a reasonable agreement between the computed and the experimental results. With significant variability in the experimental data, it can be hard to conclude the effect of water on oven rise. However, the higher water recipe had marginally taller cupcakes. Higher heat transfer rate in a higher water content batter increases its temperature faster leading to an expedited material transformation to a less permeable solid foam (Figs. 19(a)–19(c)). Thus, the higher water recipe has oven rise starting earlier resulting in taller cupcakes due to higher pressure development from more trapped gas.

Surface browning of the cupcake during baking (Fig. 15) for batters of different initial moisture contents shows reasonable agreement. Unlike oven rise, the effect of water on browning is more obvious. The lower water recipe produced darker cupcakes due to the higher surface temperature (Figs. 18(a)–18(c)). Browning begins at around

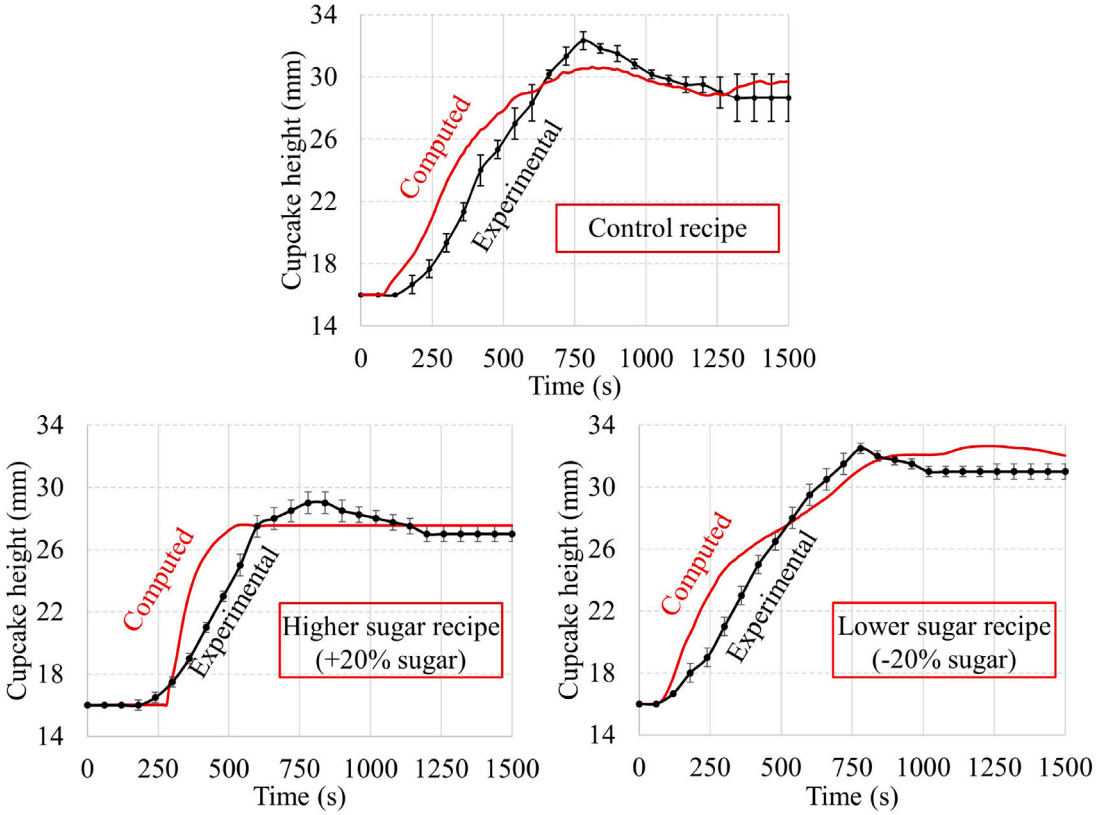

Fig. 23. Oven rise of the cupcakes during baking for batters of different sugar content.

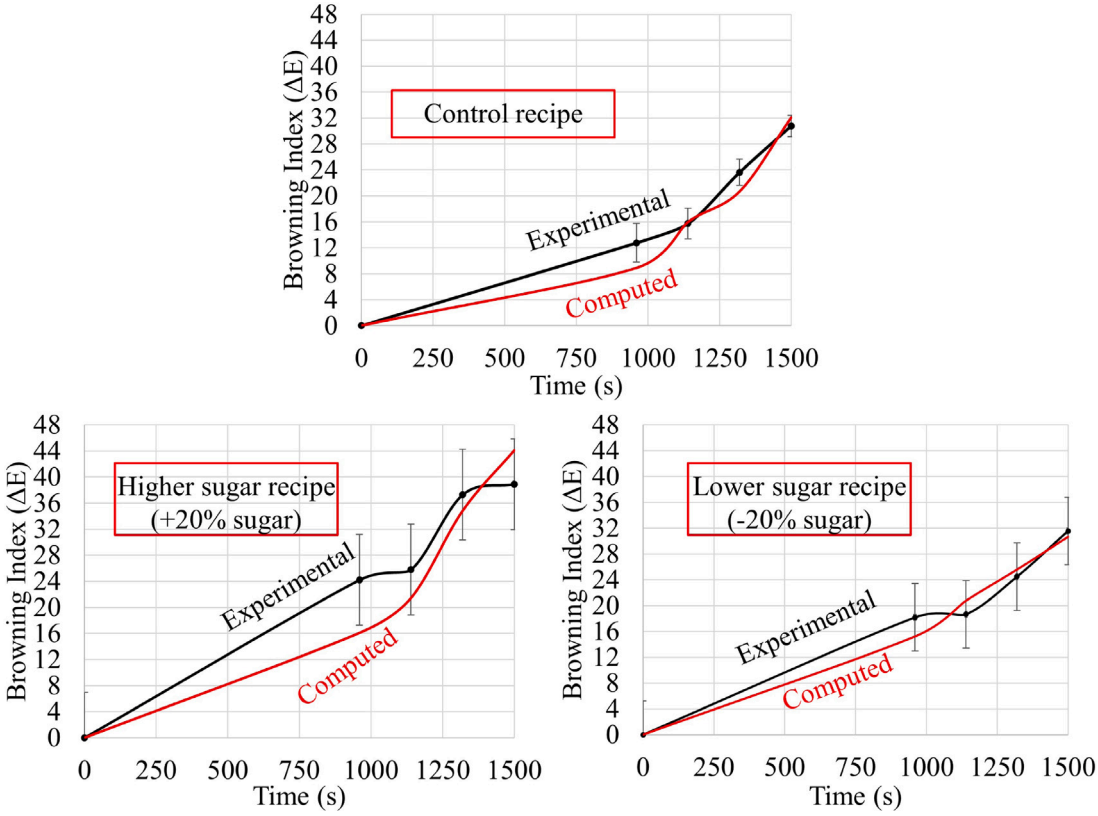

Fig. 24. Average surface browning index of the cupcakes during baking for batters of different sugar content.

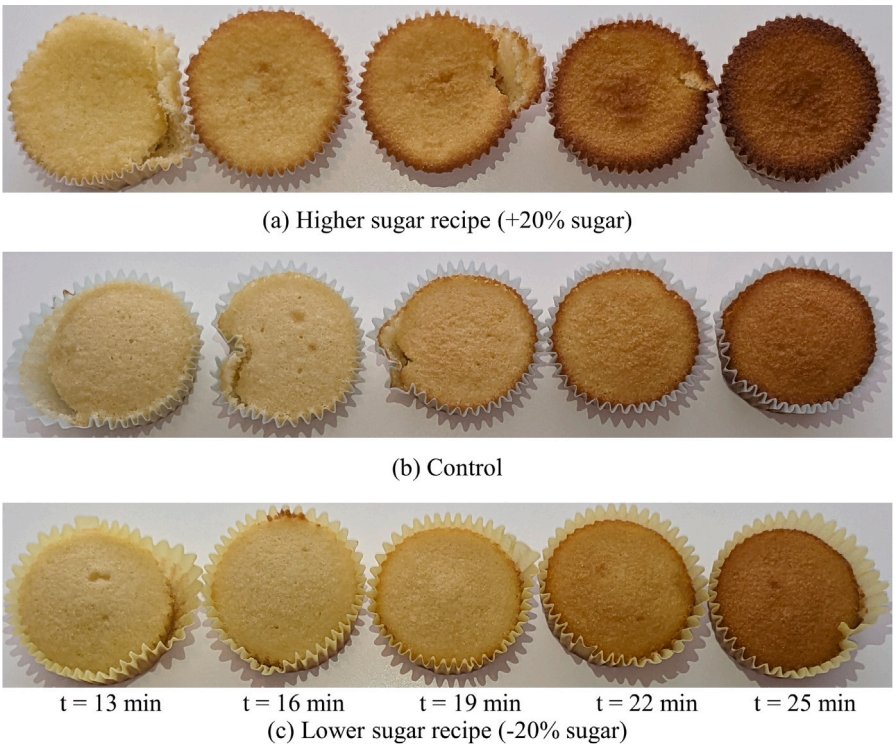

Fig. 25. Surface browning of the cupcakes during baking for batters of different sugar content.

16 min of baking. The lower water recipe has a lower evaporation rate throughout baking, leading to a higher surface temperature and, thus, higher browning (darker cupcakes) (Fig. 16).

The sequence of events relating water content to final moisture, height and color is shown in Fig. 21.

5.2.2. Role of sugar content

Change in sugar content affects moisture loss, oven rise, and browning, as shown in simulations compared with experimental results (Figs. 22–25). Among the selected recipe variations, the batter with the higher sugar content (+20% sugar) loses more water (over 30%), compared to the batter with the lowest sugar content (−20% sugar), due to evaporation during baking. The batter with the higher sugar content has a delayed material transformation (at a higher temperature) due to an increased starch gelatinization temperature (Section 2.5.4). It thus leads to delayed oven rise (Figs. 26(a)–26(c)). The delayed rise also leads to a higher heat transfer rate in the shorter cakes (shorter cakes have a smaller characteristic length and higher thermal conductivity because of less air). All this leads to a higher evaporation rate throughout baking (similar to the higher water recipe in Fig. 17(a)) and a higher moisture loss.

Fig. 23 shows oven rise (height change) during baking, as affected by sugar content, with a reasonable agreement between the computed and the experimental results. A delayed material transformation (higher permeable liquid batter to lower permeable solid as shown in Figs. 26(a)–26(c)), due to increased starch gelatinization temperature in the higher sugar batter (Section 2.5.4), leads to delayed oven rise (200 s instead of 50 s). In a higher sugar batter, delayed material transformation leads to loss of generated gas in the early stages of baking, which could aid in pressure development, which is the driving force for deformation, leading to shorter cupcakes.

Surface browning of the cupcake during baking (Fig. 24) for batters of different sugar contents shows reasonable agreement. Browning begins at around 16 min of baking. With so much experimental variation, it is not easy to comprehend the effect of sugar on browning. The higher sugar recipe had marginally darker cupcakes (Fig. 25). The shorter and drier higher sugar cupcakes reach higher surface temperatures (similar to the low water recipe) and thus more browning (Fig. 25). More sugar available for caramelization also causes increased browning.

The sequence of events relating sugar content to final moisture, height and color is shown in Fig. 27.

5.2.3. Role of fat content

Fat content affects moisture loss, oven rise, and browning, as shown in simulations compared with experimental results (Figs. 28–31). Among the selected recipe variations, the batter with the higher fat content (+20% fat) loses more water (over 30%) compared to the batter with the lower fat content (−20% fat) to evaporation during baking. A higher fat content batter, like a higher sugar content batter, has delayed material transformation (due to increased starch gelatinization temperature) and hence a delayed oven rise and shorter cakes (Section 2.5.4). Thus, the higher fat batter has a higher evaporation rate throughout baking (similar to the higher water recipe), leading to a higher moisture loss.

Fig. 29 shows oven rise (height change) during baking, as affected by fat content, with a reasonable agreement between the computed and the experimental results. A delayed material transformation in the higher fat batter leads to the delayed formation of the outer low permeability layer and, thus, delayed oven rise. More of the generated gas leaves the batter without aiding pressure development, leading to shorter cakes.

Surface browning is affected by the batter fat content (Figs. 30,31). Computed and experimentally measured (average of three replicates) browning shows similar trends (Fig. 30). With so much experimental variability, the effect of fat on browning is not obvious. However, the shorter and drier higher-fat cupcakes, similar to the lower water recipe, have higher surface temperatures (shorter cupcakes have a smaller characteristic length and higher thermal conductivity due to less air) and thus higher browning (Fig. 31).

Relationships between fat content and final variables are captured in Fig. 32.

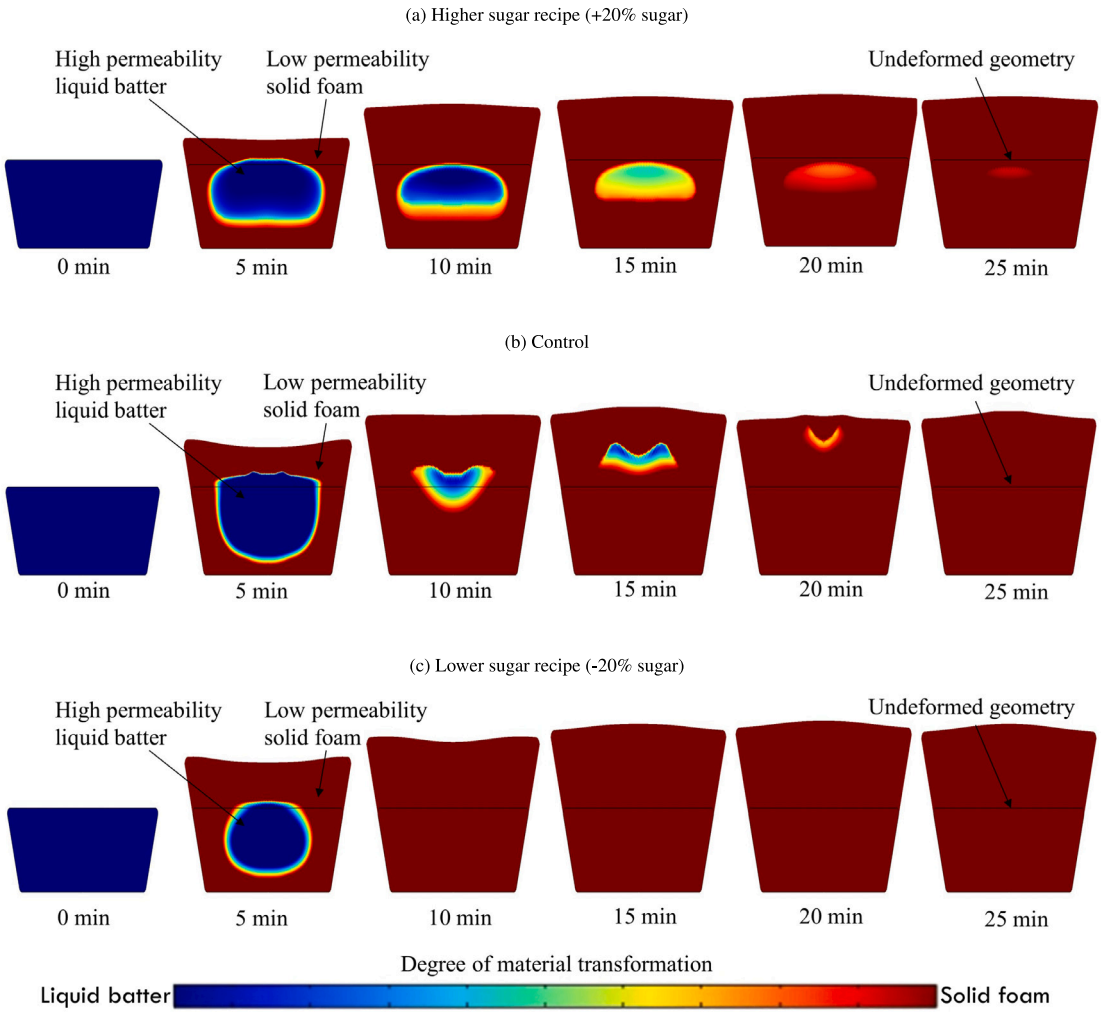

Fig. 26. Material transformation from high permeability liquid batter to low permeability solid foam inside the cupcake during baking for batters of different sugar content.

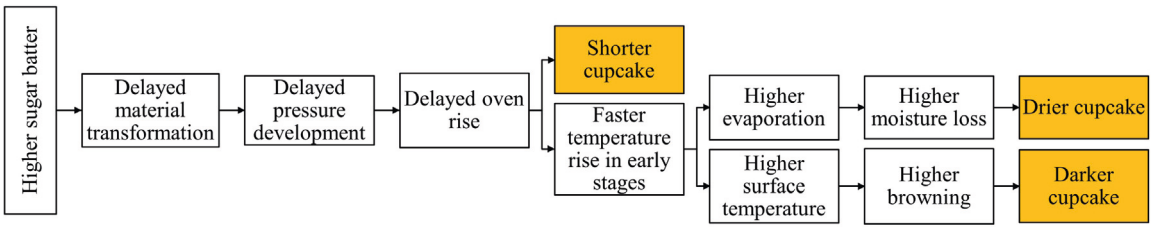

Fig. 27. Role of sugar on moisture loss, oven rise, and browning of cupcakes, summarizing the mechanistic understanding developed using model and experiments. The effect of sugar on browning is not obvious from experiments.

6. Conclusions

Using a multicomponent, multiphase transport model in a deformable porous medium, we could mechanistically explain the effects of ingredients such as initial water, fat, and sugar on oven rise, color, and moisture loss quality indicators. The insight obtained is comprehensive and novel during baking from a liquid batter to a solid foam, including spatial and temporal information, temperature, water content, gas pressure, dimension change, evaporation front, gas permeability, degree of material transformation, and color development.

Increasing water content increases thermal diffusivity, leading to faster temperature rise and higher evaporation rate, expediting oven rise but lower surface temperature and thus less browning. Increasing sugar and fat content of the batter delays the batter-to-foam material transformation (increased starch gelatinization temperature), causing more of the generated vapor to leave the batter early in baking, instead of contributing to the pressure development that occurs in the presence of the foam. This delayed transformation leads to shorter and drier cupcakes. This smaller characteristic length (because shorter) and decreased evaporation (because drier), in turn, increases the surface temperature, making the cupcakes darker.

Thus, changes inside the cupcake during baking primarily hypothesized in the past are now understood confidently. This understanding extends to other processes involving heat transfer, evaporation and gas generation, and deformation, as in cookie or biscuit baking, bread baking, and other baked goods. The first principle-based mechanistic

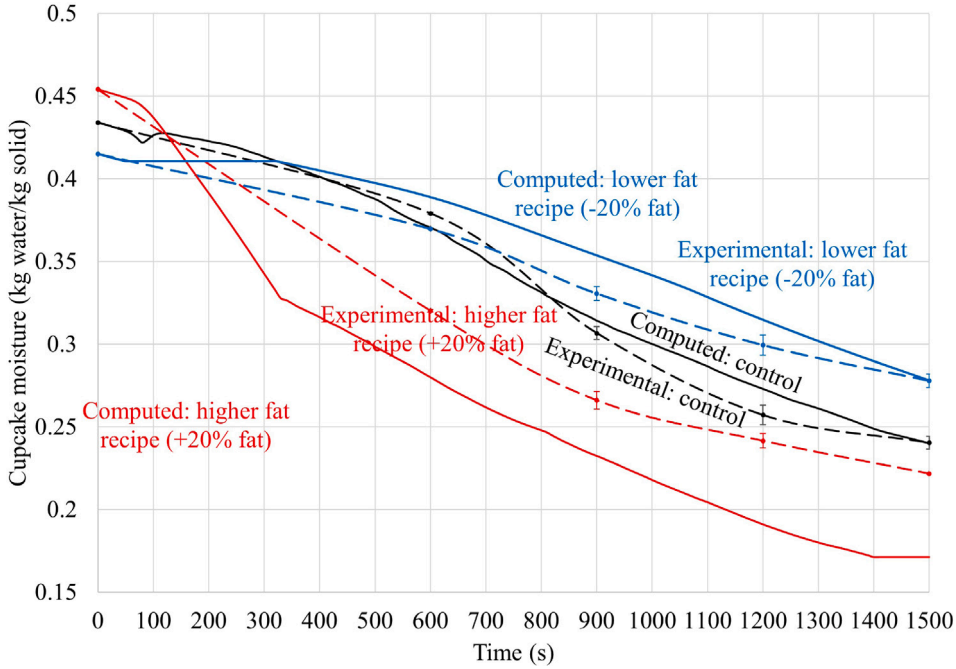

Fig. 28. Moisture content of the cupcake during baking for batters of different fat content.

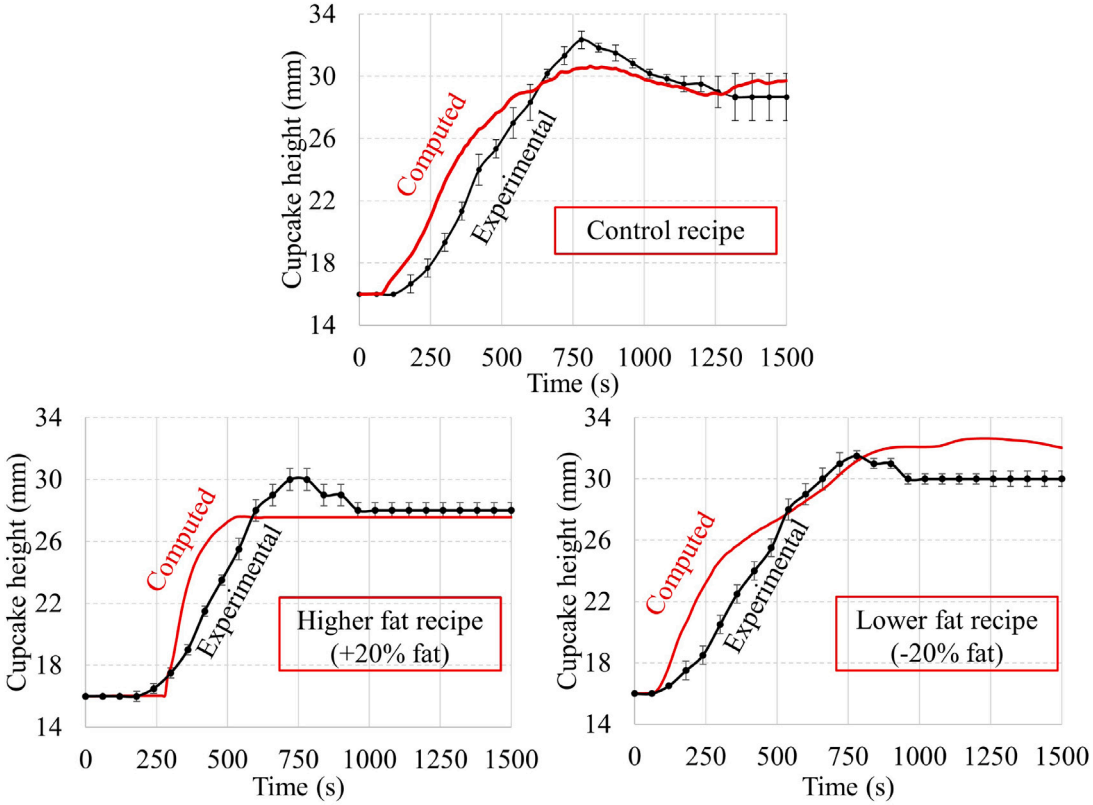

Fig. 29. Oven rise of the cupcake during baking for batters of different fat content.

understanding of the relationship between the product and process parameters and quality factors, such as oven rise, moisture loss and color formation, allows for using the model as part of a computer-aided engineering design toolset.

As to the study's limitations, the cake baking process, from batter to foam, is complex. The model gives the general directionality, but it is difficult for the completely mechanistic model for such a complex process to predict the effects of small changes in ingredients. Future work can include more sophisticated materials characterization, property measurement, and oven parameter measurement (Seranthian, 2023). Future work can also develop surrogate models that require minimal computing resources for design.

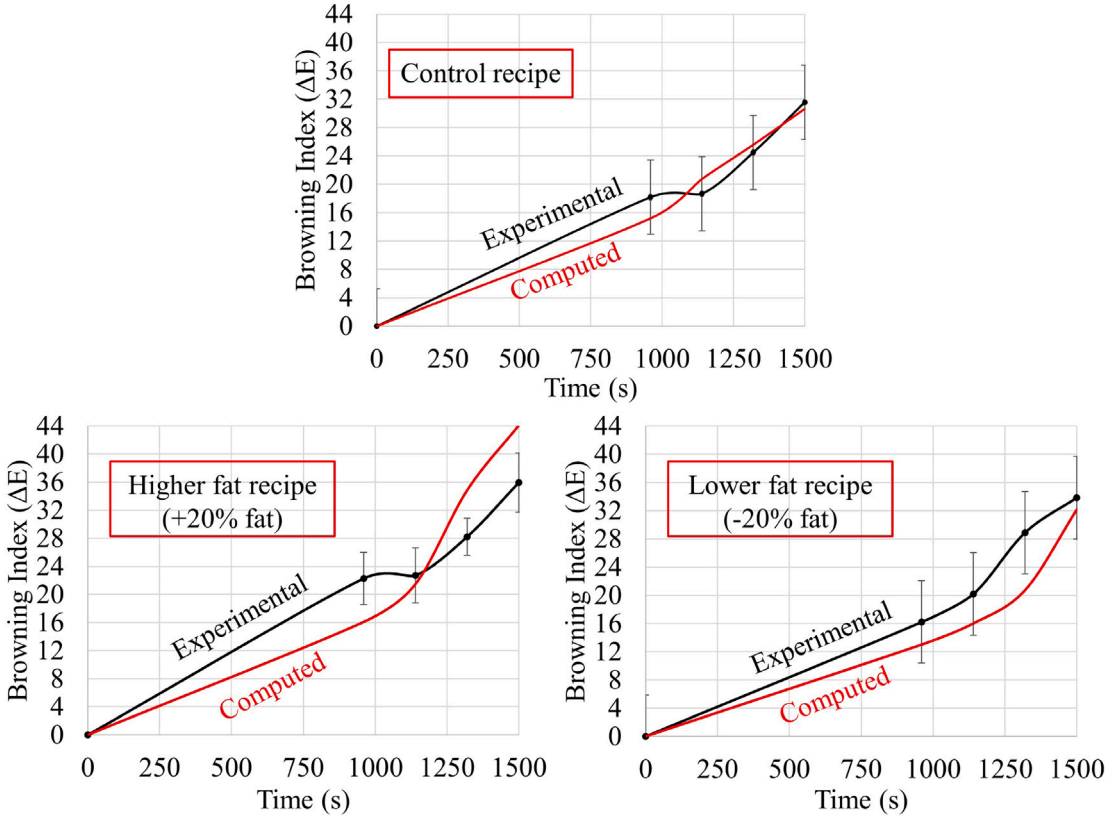

Fig. 30. Surface browning of the cupcake during baking for batters of different fat content.

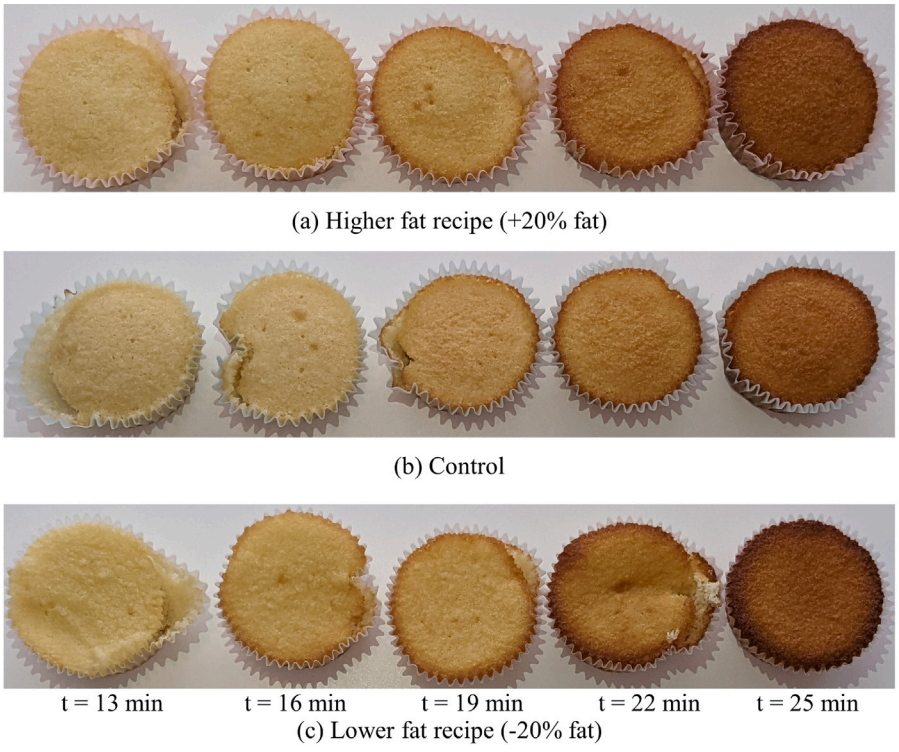

Fig. 31. Surface browning of the cupcake during baking for batters of different fat content.

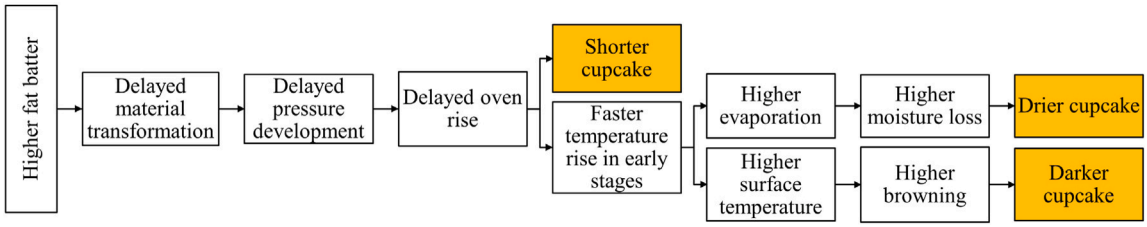

Fig. 32. Role of fat on moisture loss, oven rise, and browning of cupcakes, summarizing the mechanistic understanding developed using model and experiments. The effect of fat on browning is not obvious from experiments.

Nomenclature

Symbol	Description	Units
c	Concentration	kg/m^3
C_p	Specific heat capacity	J/kg K
C_g	Molar density	kmol/m^3
$D_{eff,g}$	Vapor diffusivity in air	m^2/s
$D_{w,cap}$	Capillary diffusivity	m^2/s
E	Elastic modulus	N/m^2
$\mathbf{E}$	Green–Lagrange strain tensor	
$\mathbf{F}$	Deformation tensor	
h_t	Heat transfer coefficient	W/m^2 K
h_m	Mass transfer coefficient	m/s
$\dot{I}$	Rate of evaporation	kg/m^3 s
$\mathbf{I}$	Identity tensor	
J	Jacobian	
$k_{in,i}$	Intrinsic permeability	m^2
$k_{r,i}$	Relative permeability of component i	
K_{evap}	Evaporation rate constant	1/s
m	Overall mass fraction	
M	Moisture content (dry basis)	kg water/ kg dry solid
M_i	Molecular weight of component i	kg
$\vec{n}$	Mass flux	kg/m^2 s
$\vec{N}$	Unit normal	
p	Pressure	Pa
r	Radius	m
S_i	Saturation of fluid phase i	
$\mathbf{S}$	Piola–Kirchhoff stress tensor	Pa
t	Time	s
T	Temperature	°C
$\vec{u}$	Displacement	m
$\vec{v}$	Velocity	m/s
x_i	Mole fraction of component i in gas phase	
V	Volume	m^3
Greek symbols		
ρ	Density	kg/m^3
λ	Latent heat of vaporization	J/kg
ω_i	Mass fraction of component i	
ϕ	Porosity	
σ	Stress	Pa
ϵ	Strain	
Subscripts		
amb	Ambient	
a	Air	
cap	Capillary	
eff	Effective	
f	Fluid	
G	Ground (stationary observer)	
g	Gas	
i	ith phase	
M	Moisture	
s	Solid	
sat	Saturated	
$surf$	Surface	
v	Vapor	
w	Water	
wa	Wall	
0	At time $t = 0$	

CRediT authorship contribution statement

Kalayarasan Seranthian: Conceptualization, Formal analysis, Investigation, Methodology, Resources, Software, Validation, Visualization, Writing – original draft. **Ashim Datta:** Conceptualization, Methodology, Project administration, Resources, Supervision, Writing – review & editing. **Aaron Clanton:** Methodology, Validation, Writing – review & editing.

Declaration of competing interest

The authors declare that they have no known competing financial interests or personal relationships that could have appeared to influence the work reported in this paper.

Data availability

The authors do not have permission to share data.

Acknowledgments

This work was carried out with partial financial support from Whirlpool Corporation. The authors wish to thank their industrial collaborators, Shaoping Shi, Lucas Baldani, Amit Khanchi, Christopher Stuart, and Nicholas Kormanik. This work used the Cornell Center for Materials Research Shared Facilities, supported through the NSF MRSEC program (DMR-1719875).

References

Andrade, R.D., Lemus, R., Perez, C.E., 2011. Models of sorption isotherms for food: uses and limitations. Vitae 18 (3), 325–334.
Antoine, M., 1888. Nouvelle relation entre les tensions et les temperatures. C. R. Held Seanc. Acad. Sci. Paris 107, 681–684.
Arik Kibar, E.A., Gönenç, İ., Us, F., 2014. Effects of fatty acid addition on the physicochemical properties of corn starch. Int. J. Food Prop. 17 (1), 204–218.
Basu, S., Shivhare, U., Mujumdar, A., 2006. Models for sorption isotherms for foods: A review. Dry. Technol. 24 (8), 917–930.

Bean, M., WT, Y., 1978. Wheat starch gelatinization in sugar solutions. I. Sucrose: Microscopy and viscosity effects.
Bear, J., 1988. Dynamics of Fluids in Porous Media. Courier Corporation.
Beleia, A., Miller, R.A., Hoseney, R.C., 1996. Starch gelatinization in sugar solutions. Starch-Stärke 48 (7–8), 259–262.
Bennion, E.B., Bamford, G., 1997. The Technology of Cake Making. Springer Science & Business Media.
Brodie, J., Godber, J., 2000. Bakery processes, chemical leavening agents. In: Kirk-Othmer Encyclopedia of Chemical Technology. Wiley Online Library.
Cevoli, C., Panarese, V., Catalogne, C., Fabbri, A., 2020. Estimation of the effective moisture diffusivity in cake baking by the inversion of a finite element model. J. Food Eng. 270, 109769.
Choi, Y., Okos, M., 1986. Thermal properties of liquid foods.
Datta, A., 2007. Porous media approaches to studying simultaneous heat and mass transfer in food processes. I: Problem formulations. J. Food Eng. 80 (1), 80–95.
Dhall, A., Datta, A.K., 2011. Transport in deformable food materials: A poromechanics approach. Chem. Eng. Sci. 66 (24), 6482–6497.
Eliasson, A.-C., 1985. Starch gelatinization in the presence of emulsifiers. A morphological study of wheat starch. Starch-Stärke 37 (12), 411–415.
Fennema, O.R., 1996. Food Chemistry, Vol. 76. CRC Press.
Feyissa, A.H., Gernaey, K., Ashokkumar, S., Adler-Nissen, J., 2011. Modelling of coupled heat and mass transfer during a contact baking process. J. Food Eng. 106 (3), 228–235.
Godefroidt, T., Ooms, N., Pareyt, B., Brijs, K., Delcour, J.A., 2019. Ingredient functionality during foam-type cake making: a review. Compr. Rev. Food Sci. Food Saf. 18 (5), 1550–1562.
Gulati, T., Datta, A.K., 2016. Coupled multiphase transport, large deformation and phase transition during rice puffing. Chem. Eng. Sci. 139, 75–98.
Guy, R.C., Sahi, S.S., 2006. Application of a lipase in cake manufacture. J. Sci. Food Agric. 86 (11), 1679–1687.
Halder, A., Dhall, A., Datta, A., 2007. An improved, easily implementable, porous media based model for deep-fat frying: Part I: Model development and input parameters. Food Bioprod. Process. 85 (3), 209–219.
Incropera, F., DeWitt, D., 1985. Introduction to heat transfer.
Jacob, H.E., 2007. Six Thousand Years of Bread: Its Holy and Unholy History. Skyhorse Publishing Inc..
Le, C., Ly, N., Postle, R., 1995. Heat and mass transfer in the condensing flow of steam through an absorbing fibrous medium. Int. J. Heat Mass Transfer 38 (1), 81–89.
Lewis, M.J., 1990. Physical Properties of Foods and Food Processing Systems. Elsevier.
Lostie, M., Peczalski, R., Andrieu, J., 2004. Lumped model for sponge cake baking during the “crust and crumb” period. J. Food Eng. 65 (2), 281–286.
Lostie, M., Peczalski, R., Andrieu, J., Laurent, M., 2002. Study of sponge cake batter baking process. II. Modeling and parameter estimation. J. Food Eng. 55 (4), 349–357.
Martins, S.I., Jongen, W.M., Van Boekel, M.A., 2000. A review of Maillard reaction in food and implications to kinetic modelling. Trends Food Sci. Technol. 11 (9–10), 364–373.
McCabe, W.L., Smith, J.C., Harriott, P., 1993. Unit Operations of Chemical Engineering, Vol. 5. McGraw-hill, New York.
Mizukoshi, M., 1985. Model studies of cake baking. V. Cake shrinkage and shear modulus of cake batter during baking. Cereal Chem. (USA).
Mizukoshi, M., Kawada, T., Matsui, N., 1979. Model studies of cake baking. I. Continuous observations of starch gelatinization and protein coagulation during baking. Cereal Chem..
Mizukoshi, M., Maeda, H., Amano, H., 1980. Model studies of cake baking. II. Expansion and heat set of cake batter during baking. Cereal Chem. (USA).
Moldrup, P., Olesen, T., Yoshikawa, S., Komatsu, T., McDonald, A.M., Rolston, D.E., 2005. Predictive-descriptive models for gas and solute diffusion coefficients in variably saturated porous media coupled to pore-size distribution: III. Inactive pore space interpretations of gas diffusivity. Soil Sci. 170 (11), 867–880.
Nicolas, V., Vanin, F., Grenier, D., Lucas, T., Doursat, C., Flick, D., 2016. Modeling bread baking with focus on overall deformation and local porosity evolution. AIChE J. 62 (11), 3847–3863.
Purlis, E., Salvadori, V.O., 2009. Modelling the browning of bread during baking. Food Res. Int. 42 (7), 865–870.
Putseys, J.A., Derde, L.J., Lamberts, L., Ostman, E., BJOrck, I.M., Delcour, J.A., 2010. Functionality of short chain amylose- lipid complexes in starch- water systems and their impact on in vitro starch degradation. J. Agricult. Food Chem. 58 (3), 1939–1945.
Pyler, E., Gorton, L., 2008. Baking Science & Technology: Volume I: Fundamentals & Ingredients. Sosland Pub..
Sablani, S., Marcotte, M., Baik, O., Castaigne, F., 1998. Modeling of simultaneous heat and water transport in the baking process. LWT-Food Sci. Technol. 31 (3), 201–209.
Sakin, M., Kaymak-Ertekin, F., Ilicali, C., 2007. Simultaneous heat and mass transfer simulation applied to convective oven cup cake baking. J. Food Eng. 83 (3), 463–474.
Sakin, M., Kaymak-Ertekin, F., Ilicali, C., 2009. Convection and radiation combined surface heat transfer coefficient in baking ovens. J. Food Eng. 94 (3–4), 344–349.
Sakin-Yilmazer, M., Kaymak-Ertekin, F., Ilicali, C., 2012. Modeling of simultaneous heat and mass transfer during convective oven ring cake baking. J. Food Eng. 111 (2), 289–298.
Scarpa, F., Milano, G., 2002. The role of adsorption and phase change phenomena in the thermophysical characterization of moist porous materials. Int. J. Thermophys. 23 (4), 1033–1046.
Schwartzberg, H.G., Wu, J.P., Nussinovitch, A., Mugerwa, J., 1995. Modelling deformation and flow during vapor-induced puffing. J. Food Eng. 25 (3), 329–372.
Seranthian, K., 2023. Multimode Heat Transfer in a Cooking Oven with Multiphase Transport, Poromechanics, and Material Transformation in Food (Ph.D. thesis). Cornell University.
Seranthian, K., Datta, A., 2023. Dynamics of cupcake baking: Coupled multiphase heat and mass transport in a deformable porous material. Chem. Eng. Sci. 277, 118802.
Spies, R., RC, H., 1982. Effect of sugars on starch gelatinization.
Sumnu, S.G., Sahin, S., 2008. Food Engineering Aspects of Baking Sweet Goods. CRC Press.
Tanikawa, W., Shimamoto, T., 2009. Comparison of Klinkenberg-corrected gas permeability and water permeability in sedimentary rocks. Int. J. Rock Mech. Min. Sci. 46 (2), 229–238.
Ureta, M.M., Olivera, D.F., Salvadori, V.O., 2016. Baking of sponge cake: Experimental characterization and mathematical modelling. Food Bioprocess Technol. 9 (4), 664–674.
van der Lijn, J., 1976. Simulation of Heat and Mass Transfer in Spray Drying. Wageningen University and Research.
Warning, A., Verboven, P., Nicolaï, B., van Dalen, G., Datta, A.K., 2014. Computation of mass transport properties of apple and rice from X-ray microtomography images. Innov. Food Sci. Emerg. Technol. 24, 14–27.
Wilderjans, E., Luyts, A., Brijs, K., Delcour, J.A., 2013. Ingredient functionality in batter type cake making. Trends Food Sci. Technol. 30 (1), 6–15.
Zanoni, B., Peri, C., Bruno, D., 1995. Modelling of browning kinetics of bread crust during baking. LWT-Food Sci. Technol. 28 (6), 604–609.
Zhang, J., Datta, A., 2006. Mathematical modeling of bread baking process. J. Food Eng. 75 (1), 78–89.